Latest Results of Experimental Approach to Ultra-cold Beam at S-LSR

Akira Noda
Institute for Chemical Research (ICR)
Kyoto University

Present Address
National Institute of Radiological Sciences (NIRS)

at
COOL13
Mürren in Switzwerland

Co-authors

Masao Nakao#, Hikaru Souda$, Hiromu Tongu

(Kyoto ICR, Uji, Kyoto),

Hiromi Okamoto, Kazuya Osaki

(HU/AdSM, Higashi-Hiroshima),

Yosuke Yuri (JAEA/TARRI, Gunma-ken),

Kouichi Jimbo (Kyoto University, Kyoto),

Manfred Grieser (MPI-K, Heidelberg),

Zhengqi He (TUB, Beijing)

Present Address: # NIRS, $Gunma-University

Contents

1. **Electron Cooling**
   1D Ordering of 7 MeV proton beam
   Bio-medical Vertical Irradiation Port with Short Bunch

2. **Experimental Demonstration of Active Multi-dimensional Laser Cooling of 40 keV $^{24}Mg^{+}$ ion beam**

3. **Improvement of Laser Cooling Efficiencynby suppression of IBS with Scraping**

4. **Comparison of Attained Temperatures**

Compact Cooler Ring S-LSR

－Circumference 22.56m

－Straight Section Length 1.86m

E-cooling modes

- Protons 7MeV (Ee=3.8keV)

- Laser cooling
  - $^{24}Mg^{+}$ 40 keV (λ=282 nm)

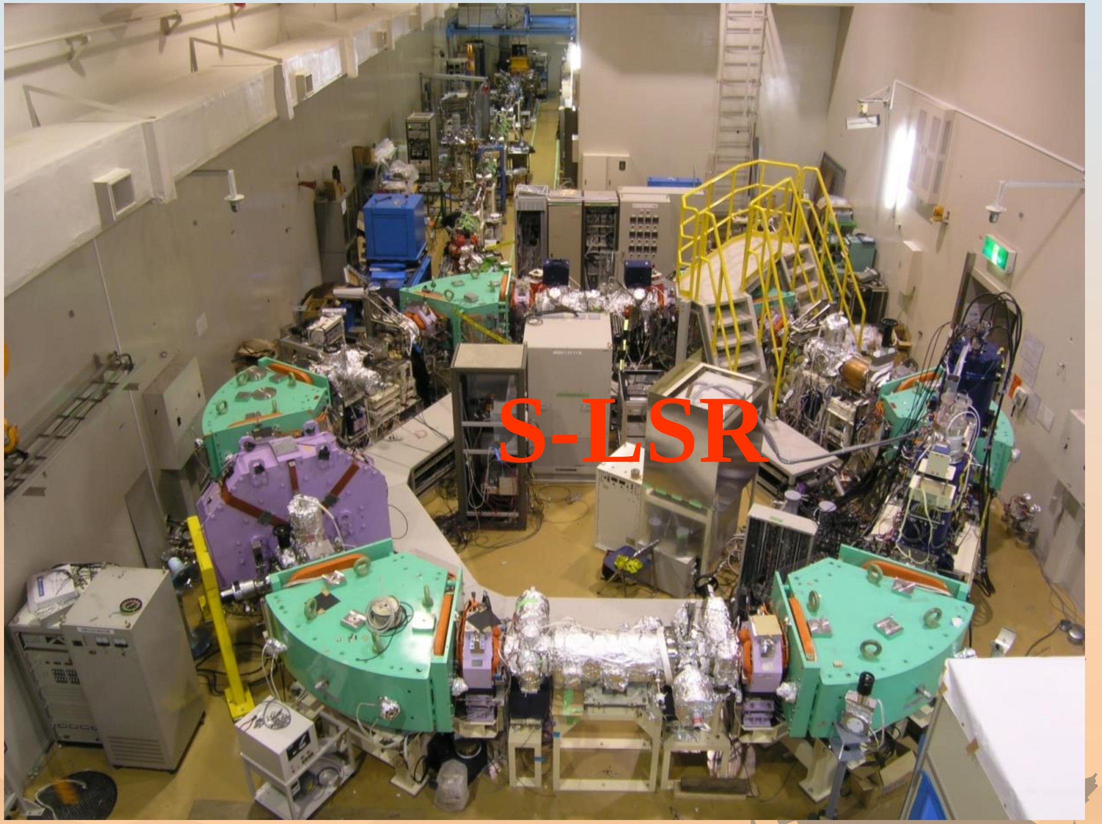

In operation since October, 2005

Main Parameters of S-LSR

Circumference	22.557 m
Average radius	3.59 m
Length of straight section	1.86 m
Number of periods	6
Betatron Tune	
Crystalline Mode	Normal Operation Mode
1.45 (H) , 1.44 (V)	1.872(H), 0.788 (V): EC
	2.068(H), 1.105, 1.070 (V): LC
Bending Magnet	(H-type)
Maximum field	0.95 T
Curvature radius	1.05 m
Gap height	70 mm
Pole end cut	Rogowski cut+Field clamp
Deflection Angle	60°
Weight	4.5 tons
Quadrupole Magnet	
Core Length	0.20 m
Bore radius	70 mm
Maximum field gradient	5 T/m

ESR at GSI, by M. Steck

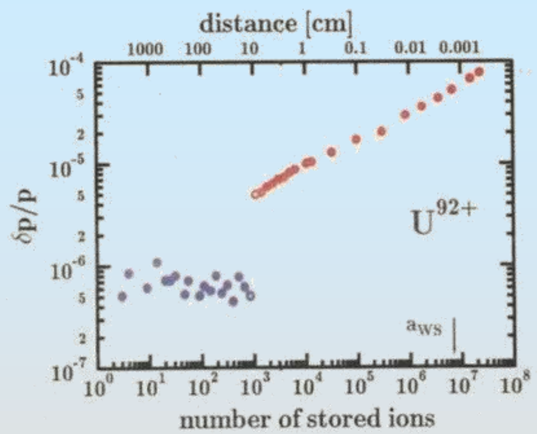

Figure 2. Experimental momentum spreads from Schottky signals *vs.* number of stored ions in the ESR for electron cooled U^{92+} ions at 240 MeV/u. a_{WS} indicates the Wigner-Seitz radius of eq.(3). (after ref. [9])

CRYRING at Stockholm, by H. Danared

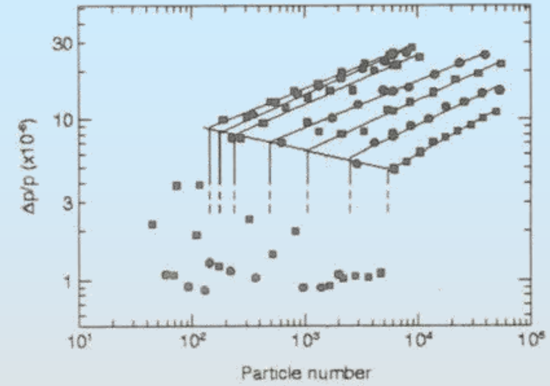

Fig. 5: Relative momentum spread as a function of particle number for the lowest seven electron densities represented in Fig. 2. The density increases from the upper left to the lower right. For each density, a line is fitted to the data points. A line is also drawn through the points corresponding to the transition to the ordered state. (The use of different symbols is just to help identifying which points belong to same electron density.)

ESR at GSI, by M. Steck

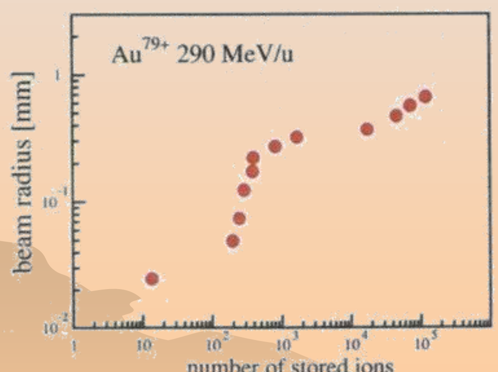

Figure 3. Beam radius measured with a beam scraper *vs.* number of stored ions in the ESR for electron cooled Au^{79+} ions at 290 MeV/u (from ref. [10]).

NAP-M at BINP, Novosibirsk by V.V. Parkhomchuk

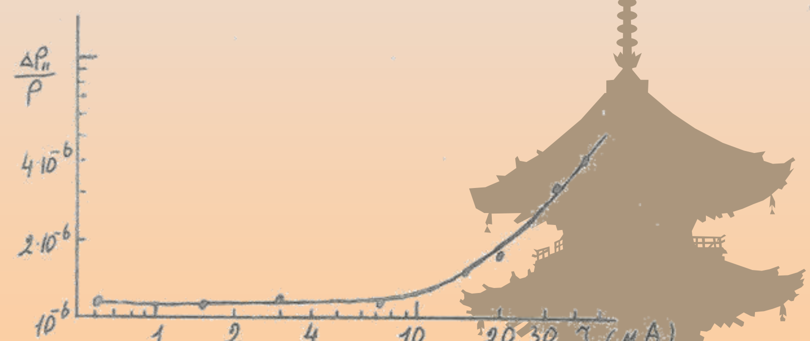

Fig. 6. The momentum spread of proton beam versus current J_p.

Ring Layout

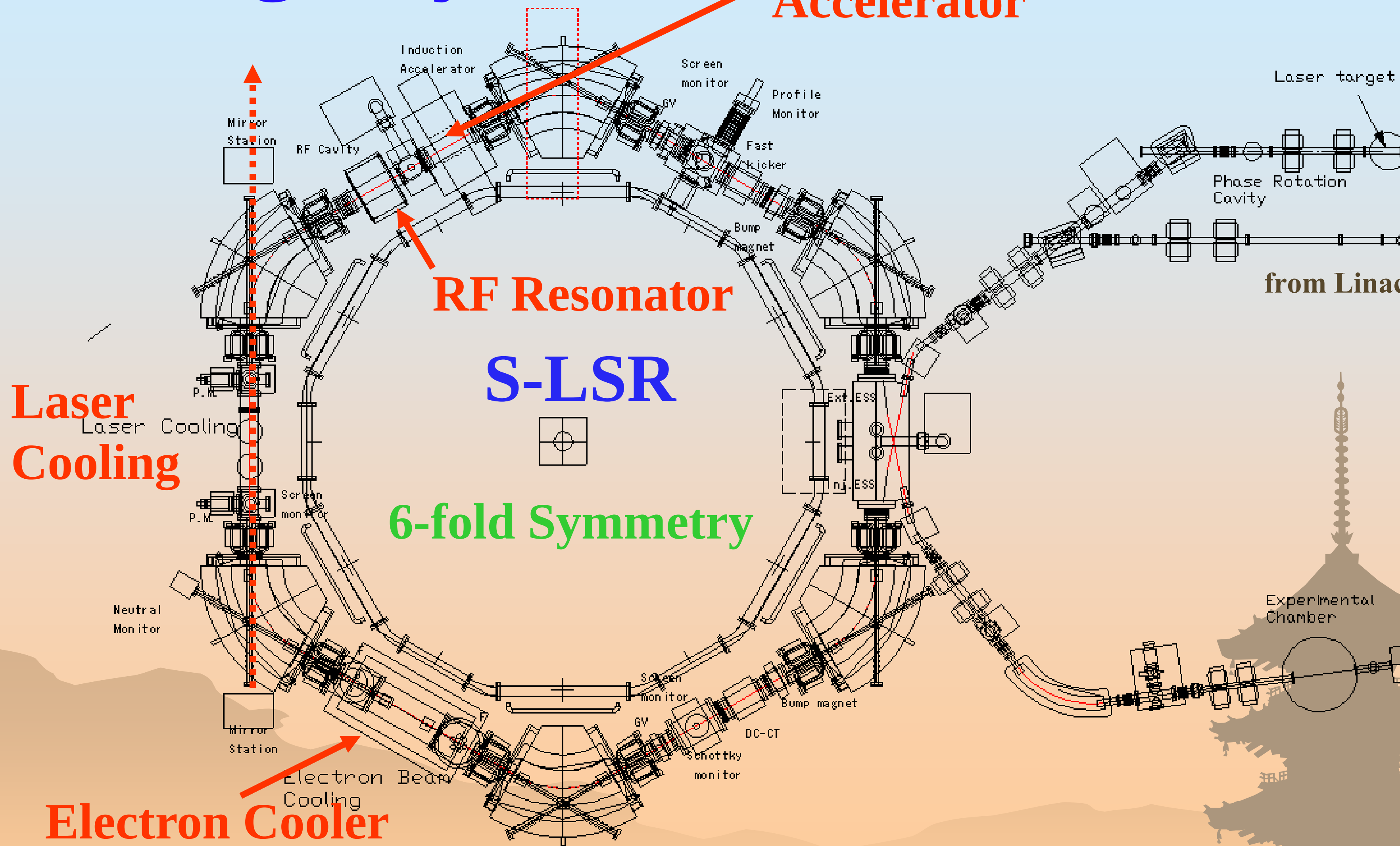
Induction
Accelerator
RF Resonator
S-LSR
6-fold Symmetry
Laser
Cooling
Electron Cooler
from Linac
Induction
Accelerator
RF Cavity
Mirror
Station
Screen
monitor
GV
Profile
Monitor
Fast
kicker
Bump
magnet
Laser target
Phase Rotation
Cavity
Laser Cooling
P.M.
Ext.ESS
Inj.ESS
Neutral
Monitor
Experimental
Chamber
Bump magnet
DC-CT
Schottky
monitor
Electron Beam
Cooling

Electron Cooler installed in S-LSR

Dr. Hicham Fadil

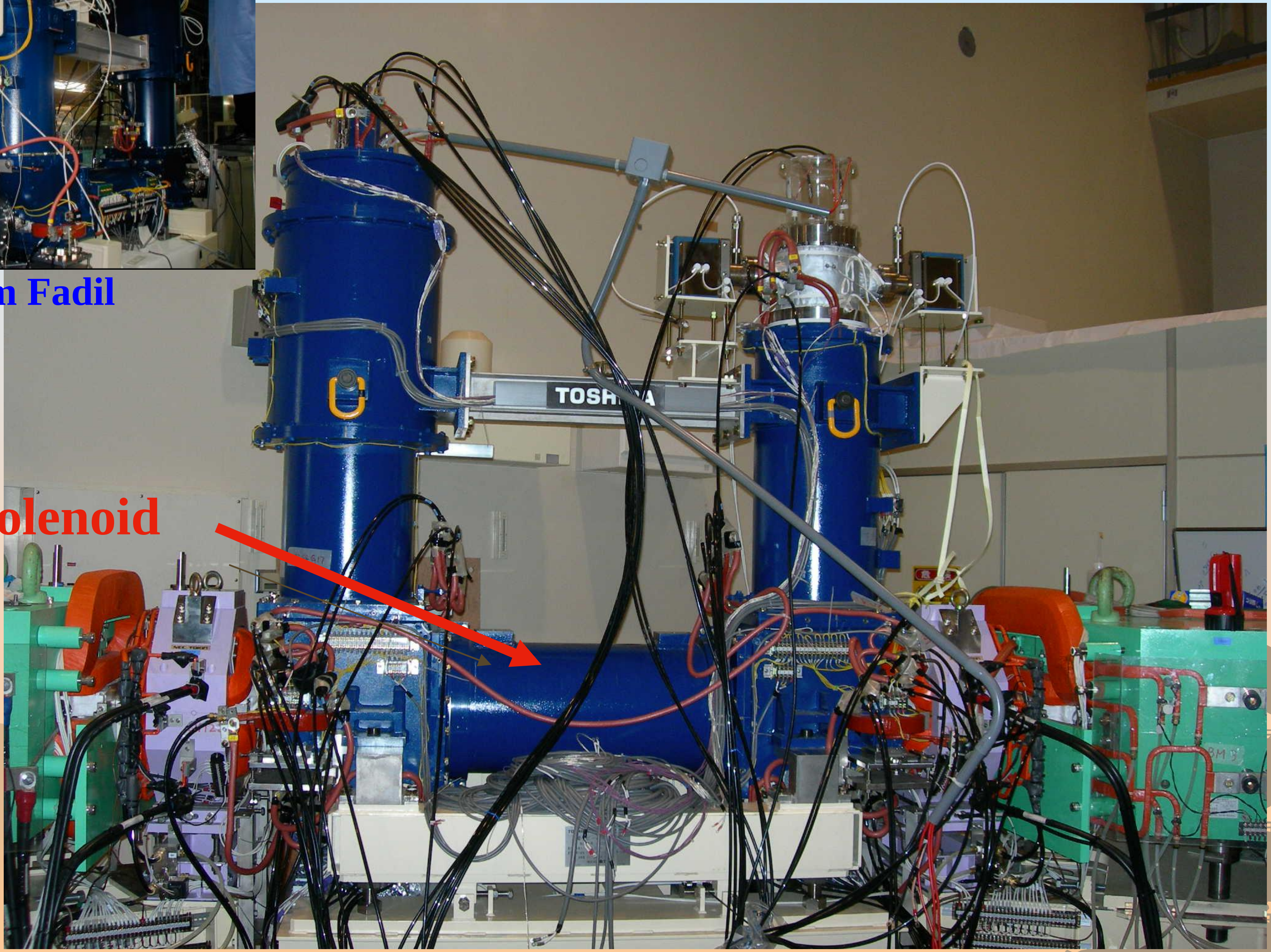

Cooler Solenoid

Simulation with Betacool predicts 1D ordering of 7 MeV proton at S-LSR -particle number of 3000-

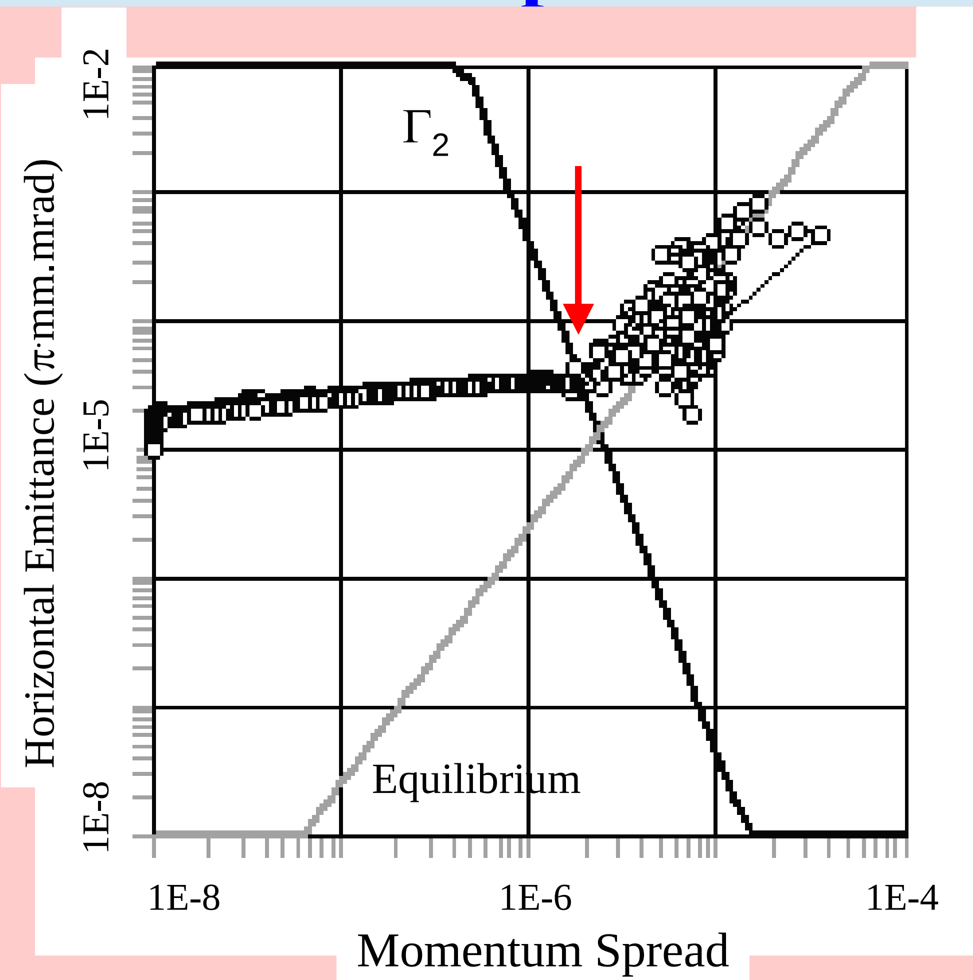

$$\Gamma_2 \equiv \frac{Z^2 e^2}{4\pi\epsilon_0 \sigma_\perp k_B T_\parallel}$$

Collaboration with JINR, Dubna by Prof. I. Meshkov and Dr. A. Smirnov et al.

Phase Transition to 1D Ordered State

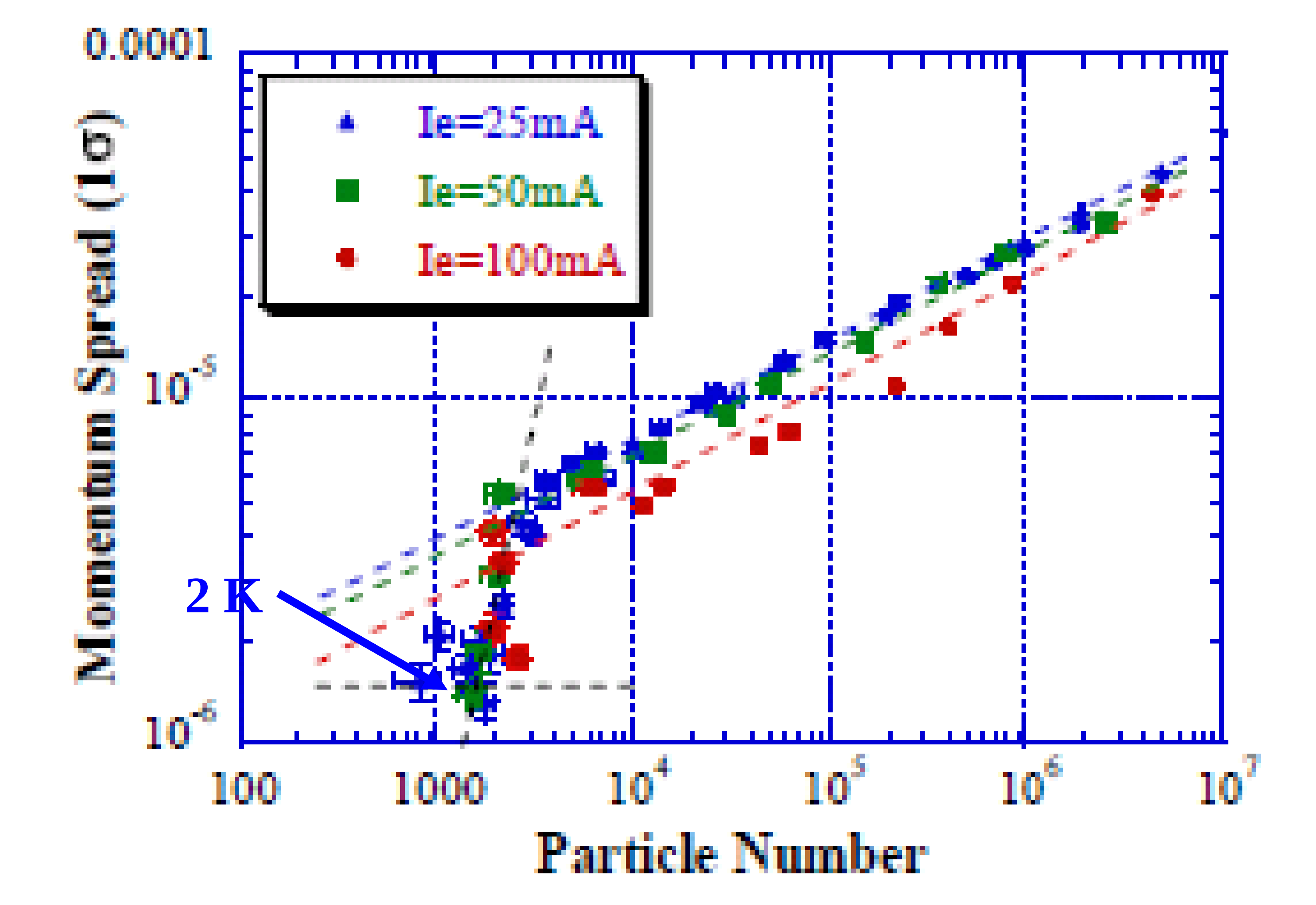

T. Shirai et al., PRL, 98 (2007) 204801

Horizontal Beam Size Reduction by Electron Cooling

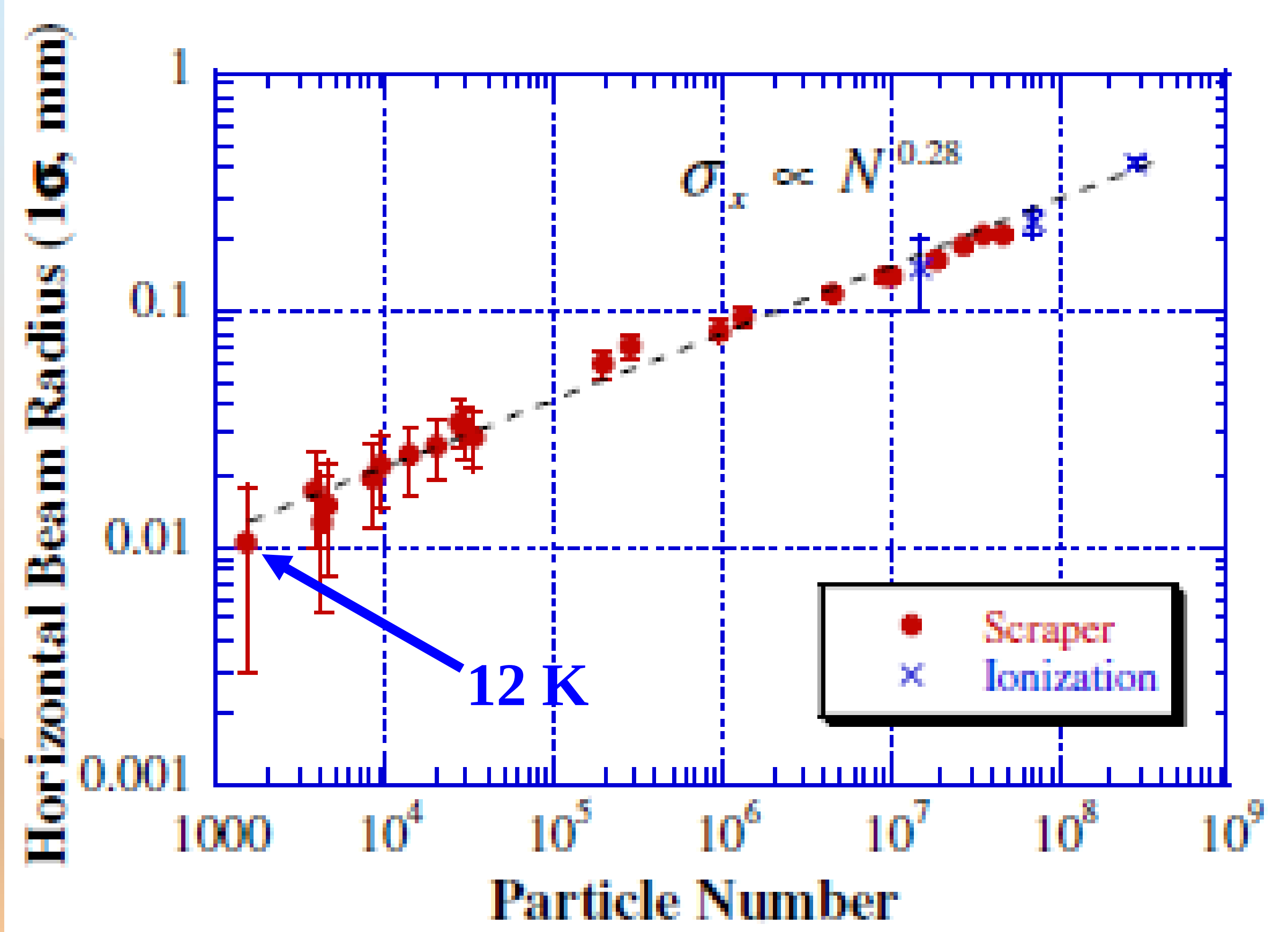

Reflection Probability of Ions made Phase Transition

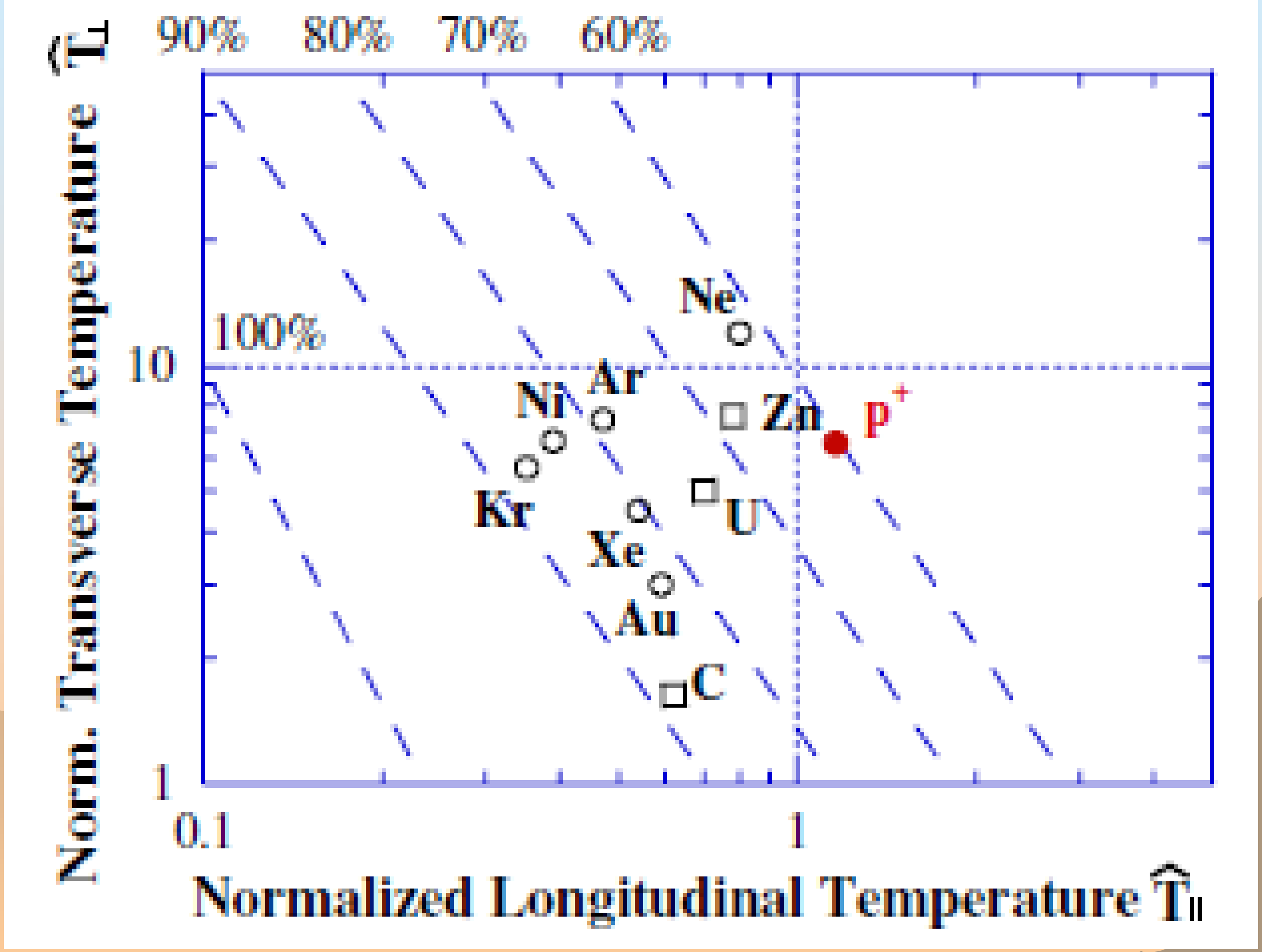

Construction of Vertical Beam Irradiation Port

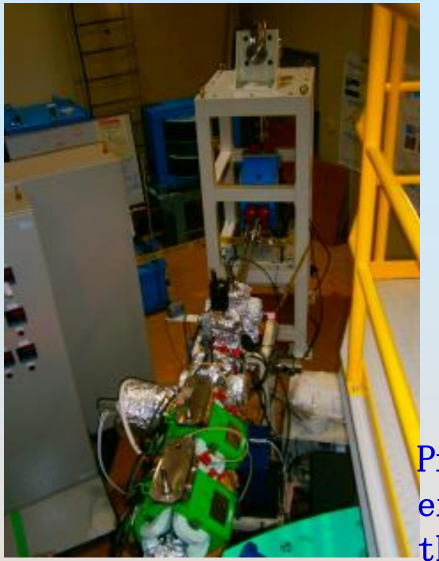

Profile measurement after extraction into air through havar foil

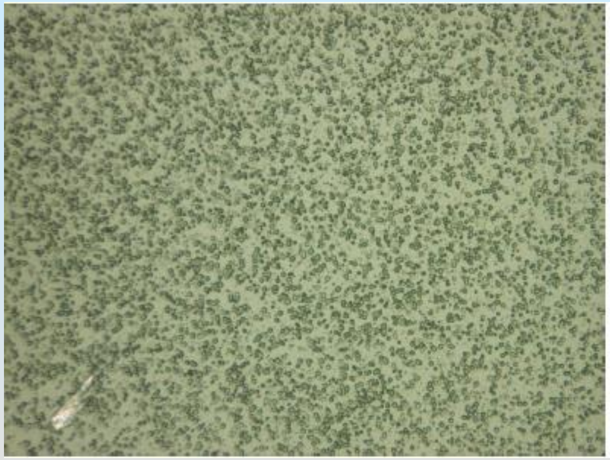

Irradiation Strength Analysis by CR39
Irradiation strength 26200 proton/mm^2

7115 pits are detected

Completed Beam Line

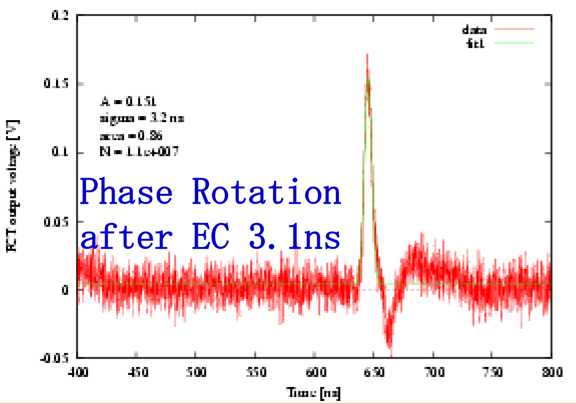

Phase Rotation after EC 3.1ns

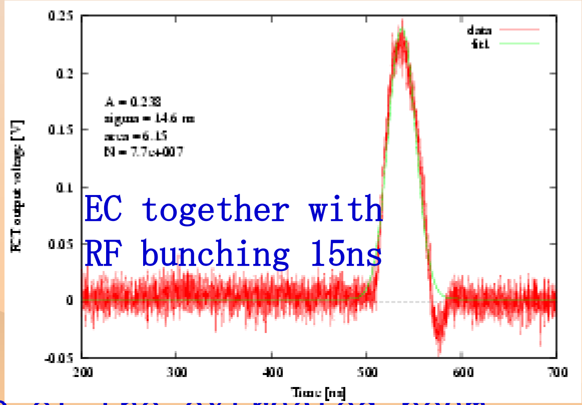

EC together with RF bunching 15ns

Time Structure of the extracted beam

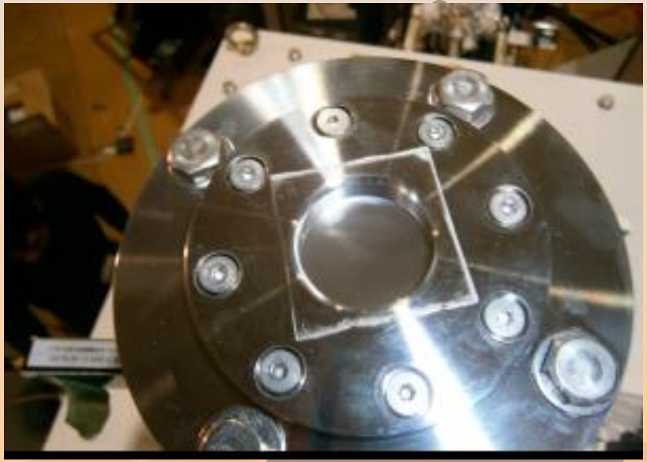

Extracted into air through havar foil of 10μm thickness

Approach to much Lower Temperature by Laser Cooling Applied for 40 keV $^{24}Mg^{+}$ Ion Beam

Simulation by H. Okamoto et al.

Expectation from Simulation

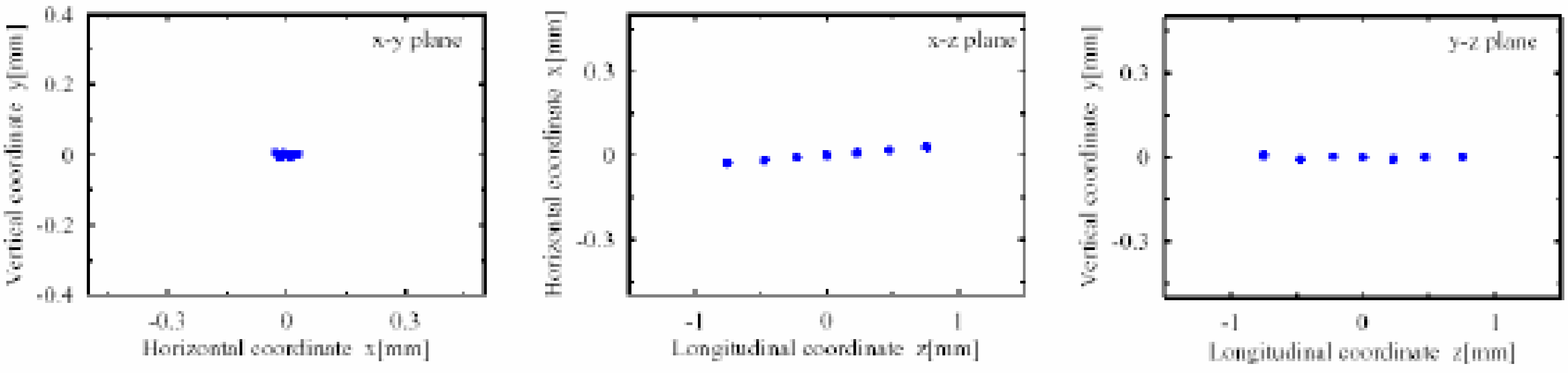

(a) 1D ordering

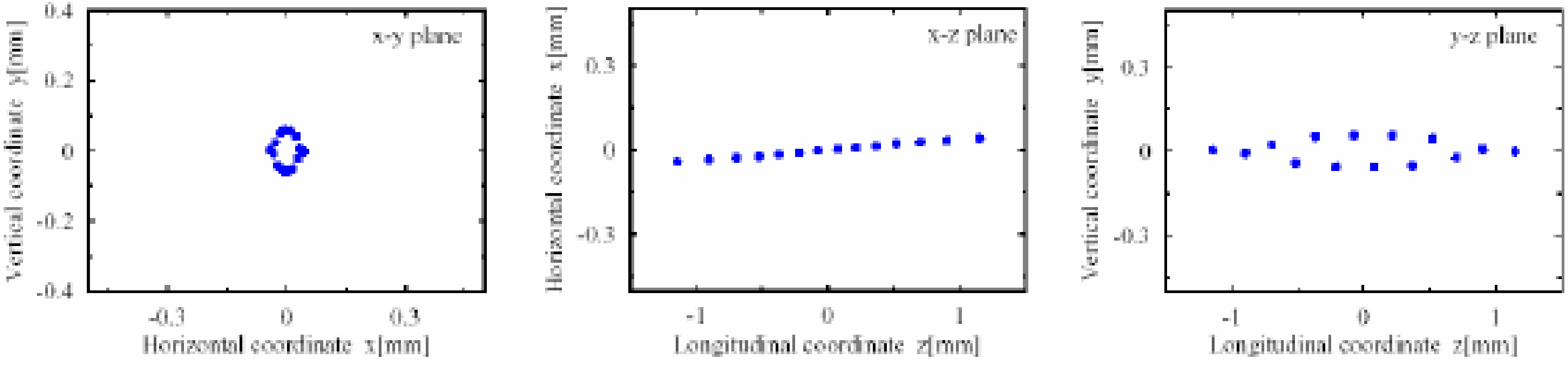

(b) 2D zigzag structure

Crystalline Beam in Circular RFQ, PALLAS

T. Schatz, U. Schramm, D. Habs:, Nature, 412, 717 (2001)

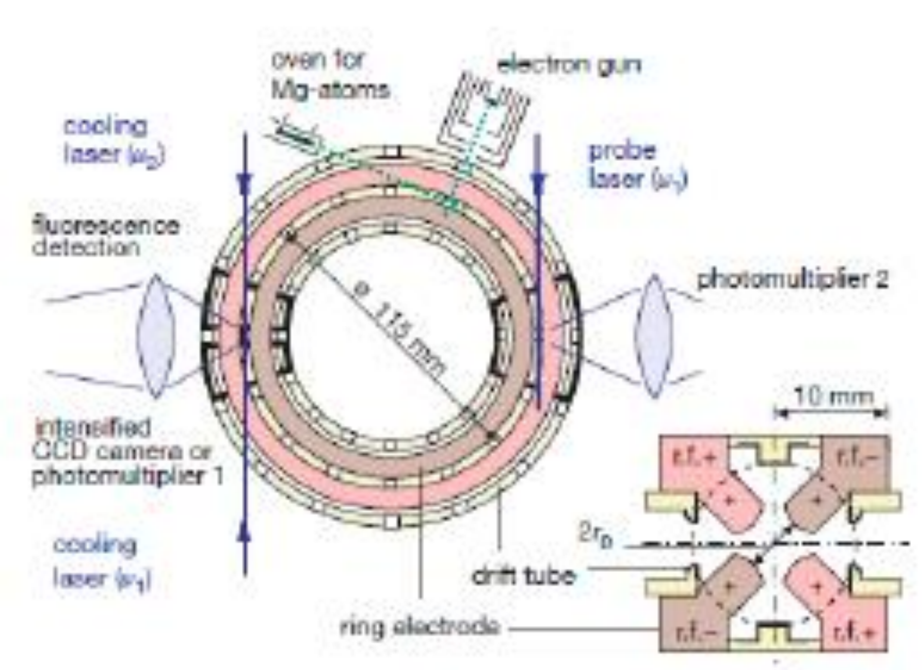

Structure of Circular RFQ, PALLAS

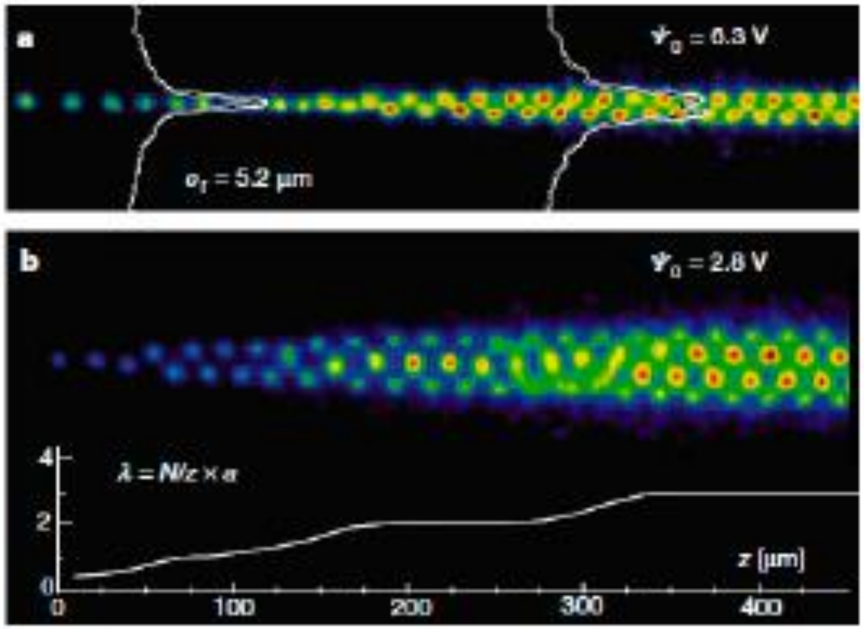

Images of ion crystals at rest in PALLAS

Excited States of Mg Ion

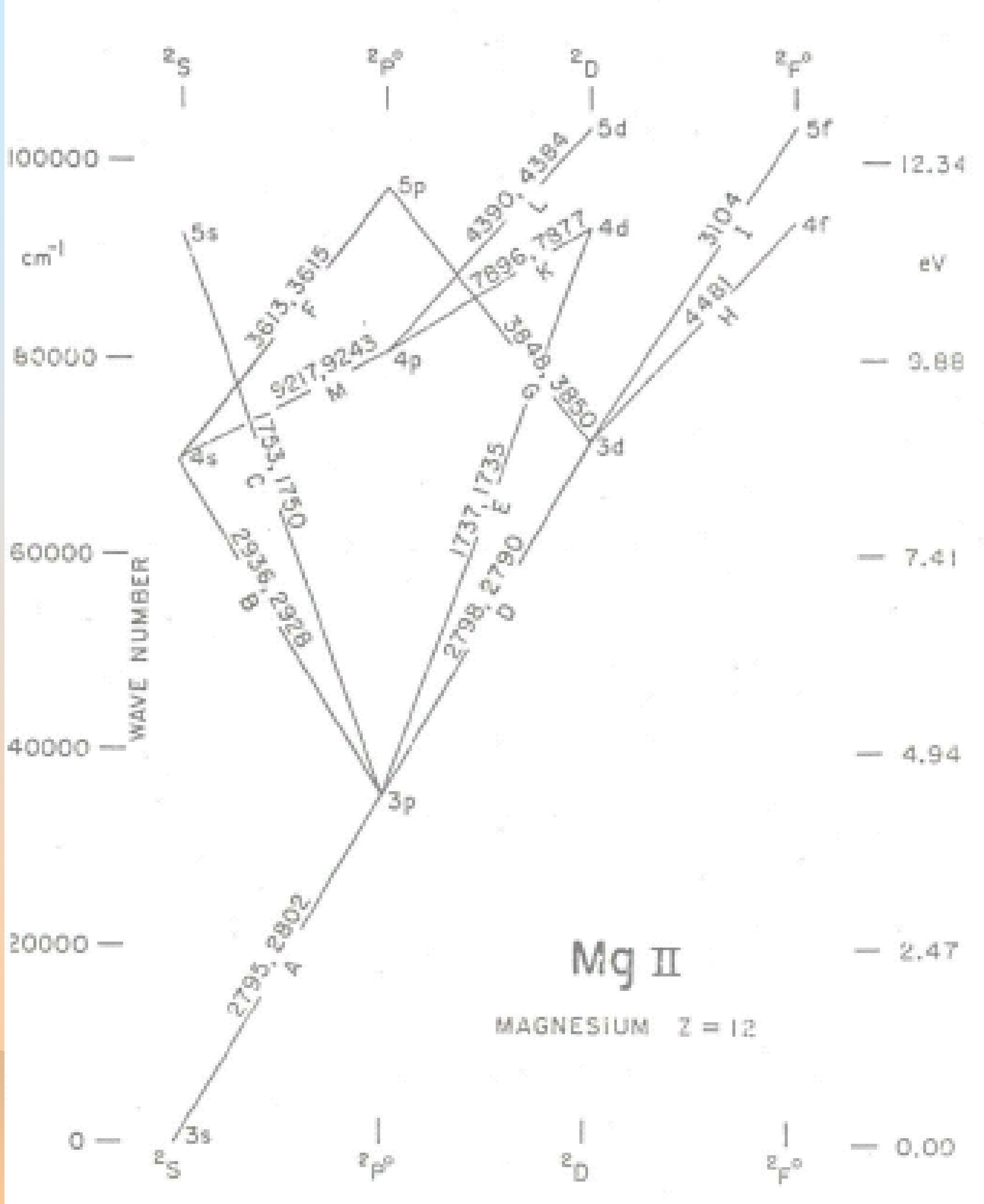

Principle of Laser Cooling (Longitudinal)

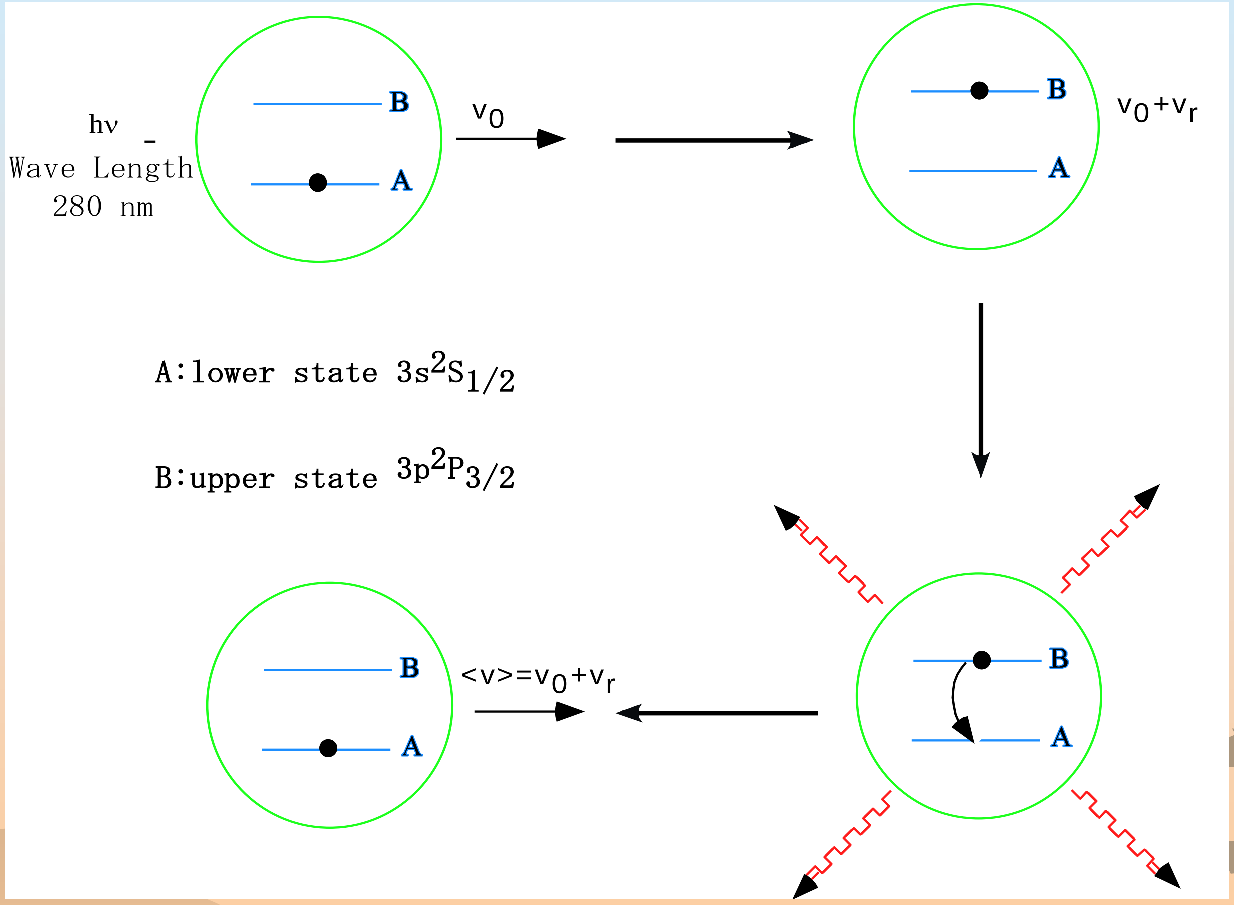

Block Diagram of Laser Cooling at S-LSR

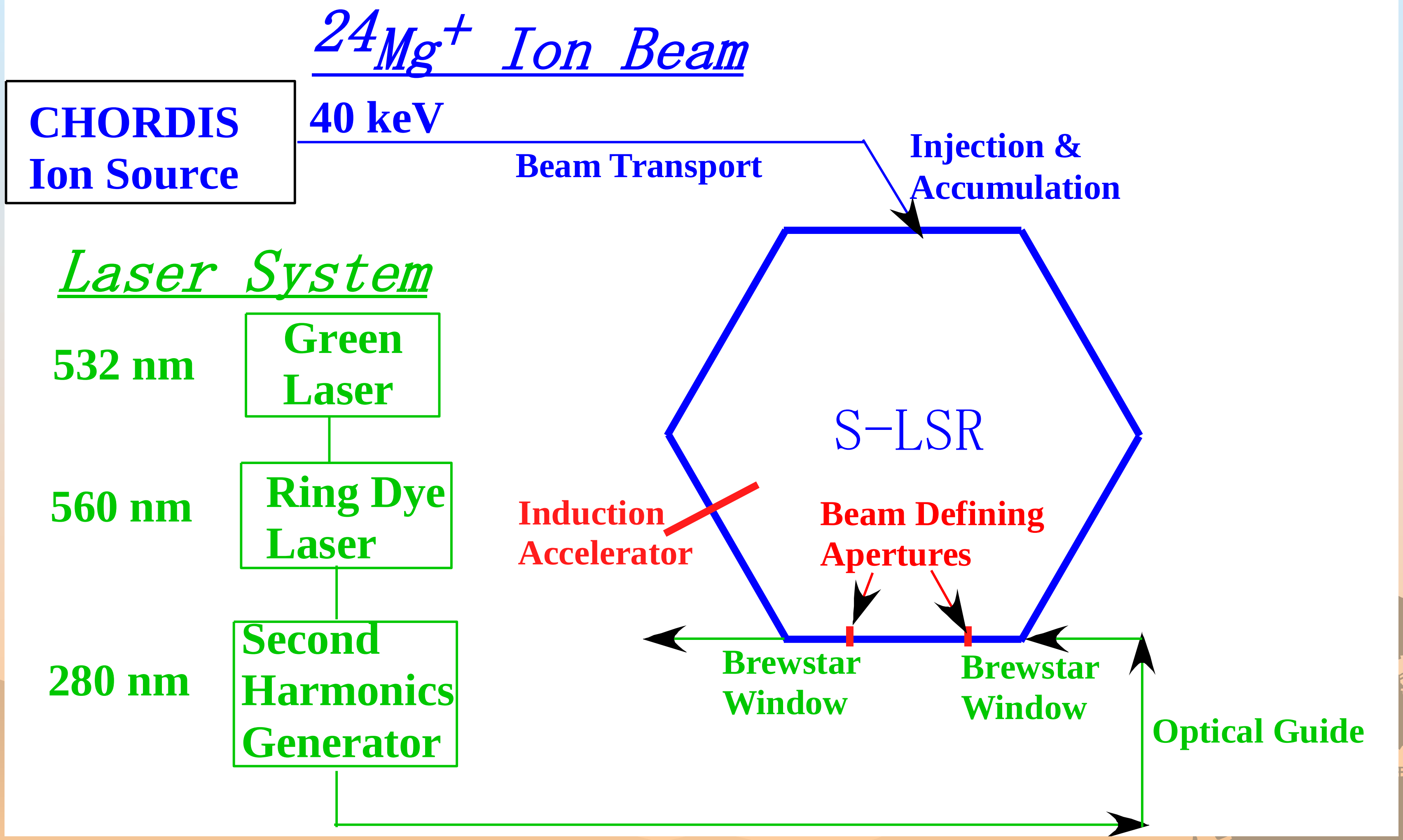

$^{24}Mg^{+}$ Ion Source (40 keV)

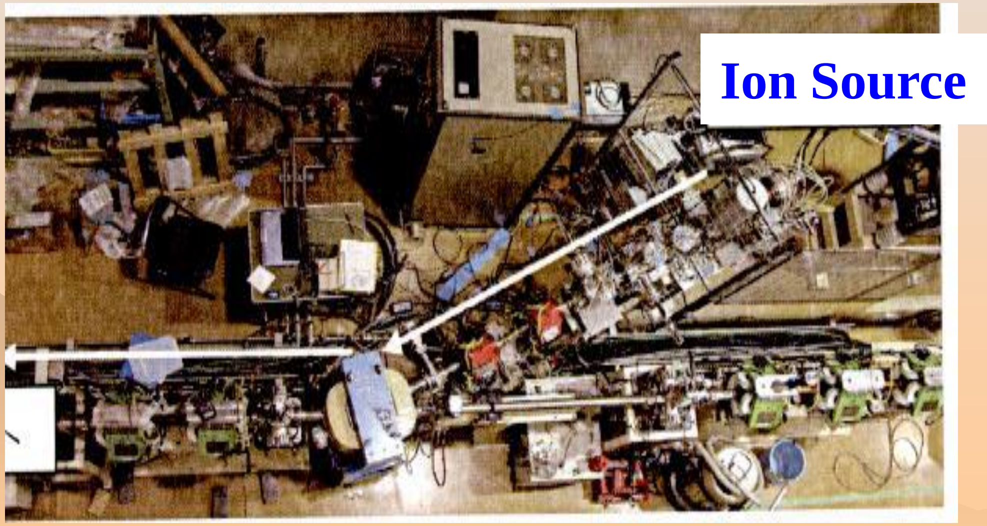

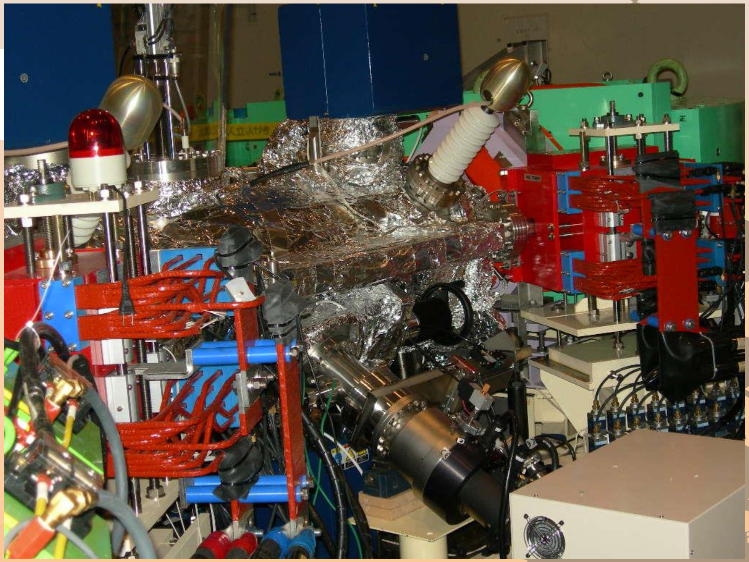

COD Correction System of S-LSR

H. Souda et al., N.I.M. A597 (2008), pp160-165

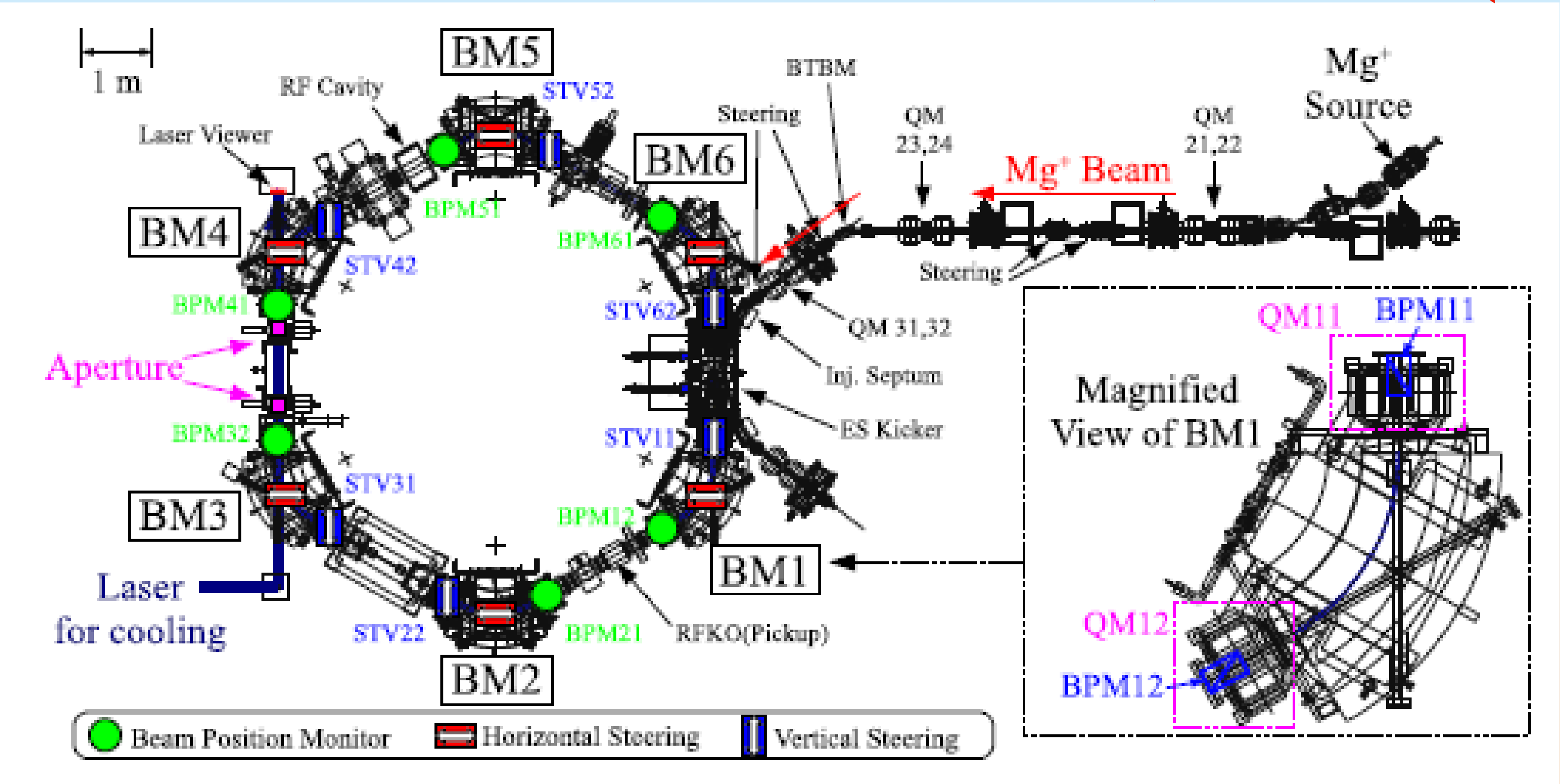

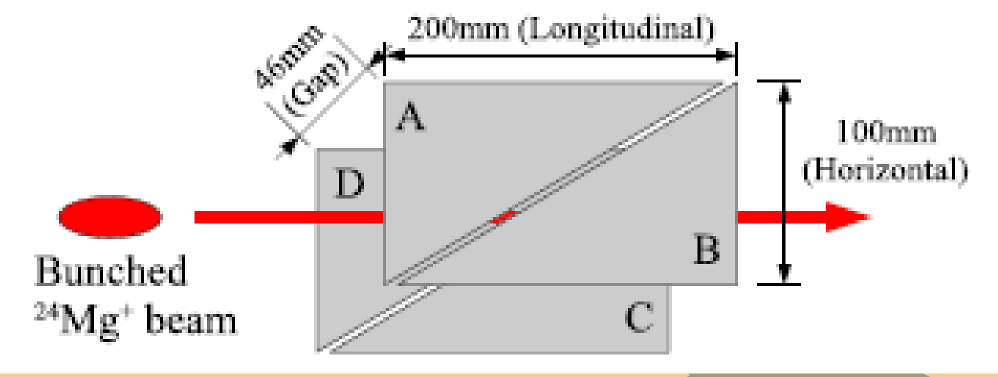

COD Correction and Beam Life of Mg Ion

H. Souda et al., N.I.M. A597 (2008), pp160-165

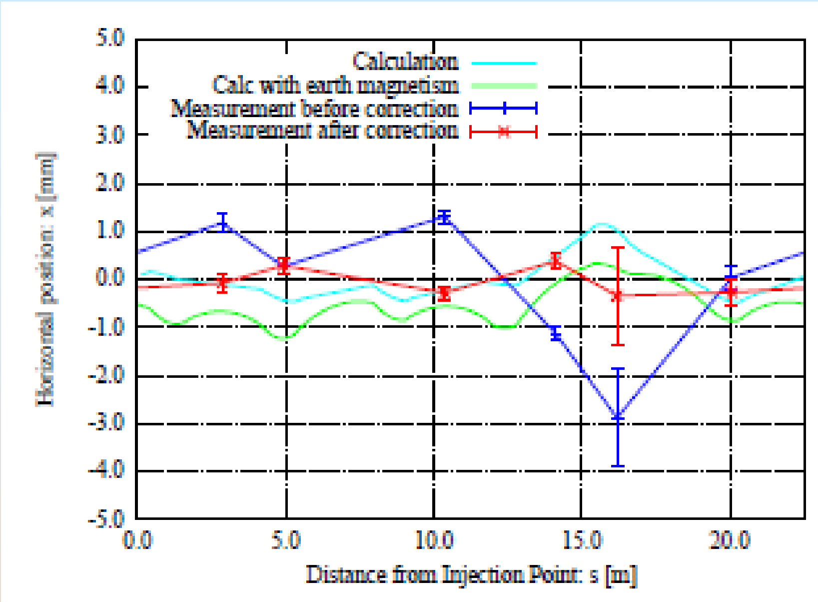

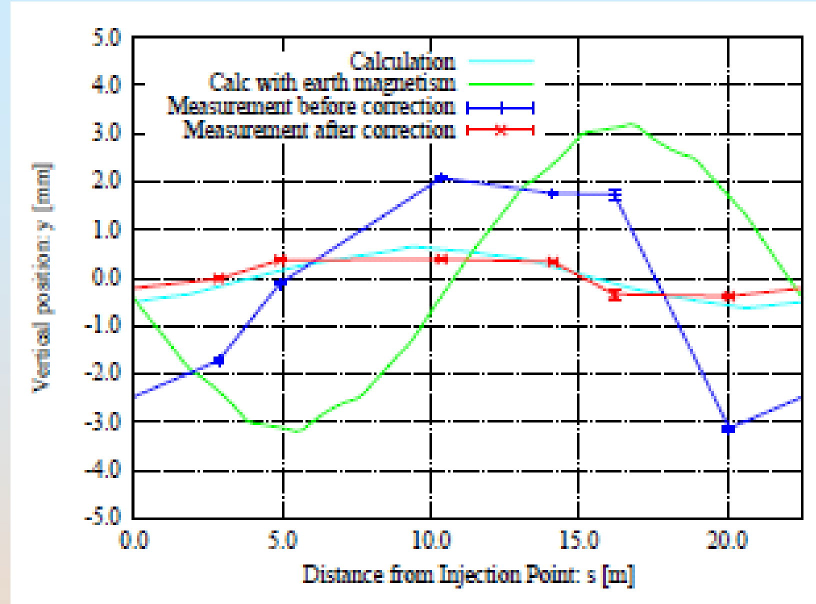

Beam Life of 40 keV $^{24}Mg^{+}$ Ion for Various Operation Points

ν_x	ν_y	Beam Life
2.068	1.069	7.5 s (10.3s)
2.115	0.724	14.2 s
1.53	1.34	14.1 s
1.642	1.198	13.5 s

Laser System for Cooling

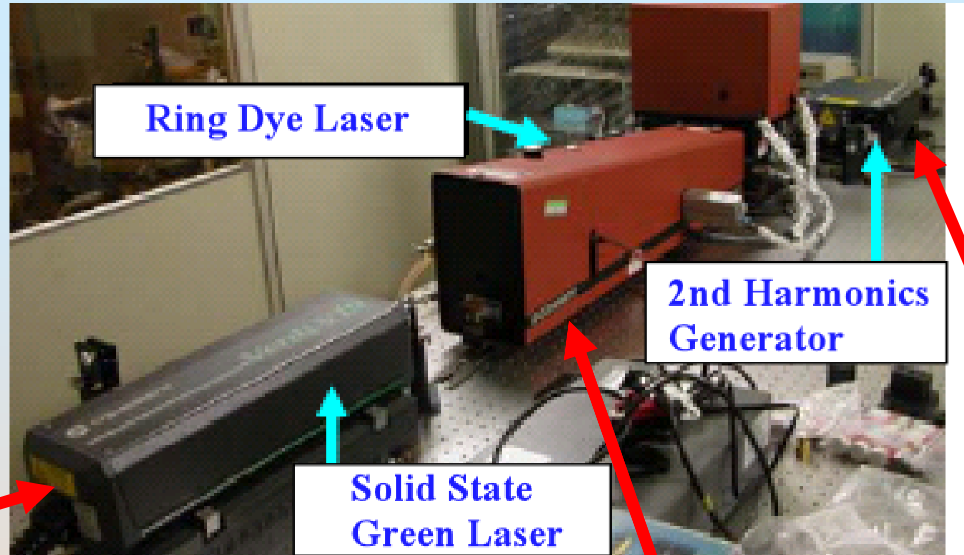

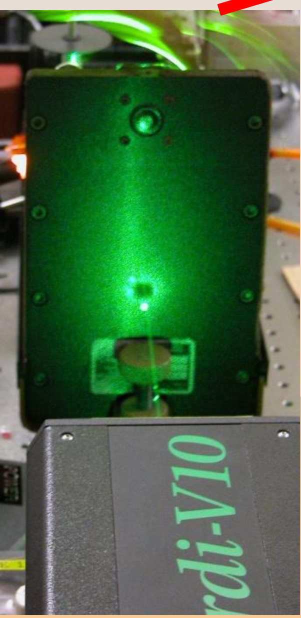

Laser Cooling Section of S-LSR

Induction Accelerator

Window for Laser port

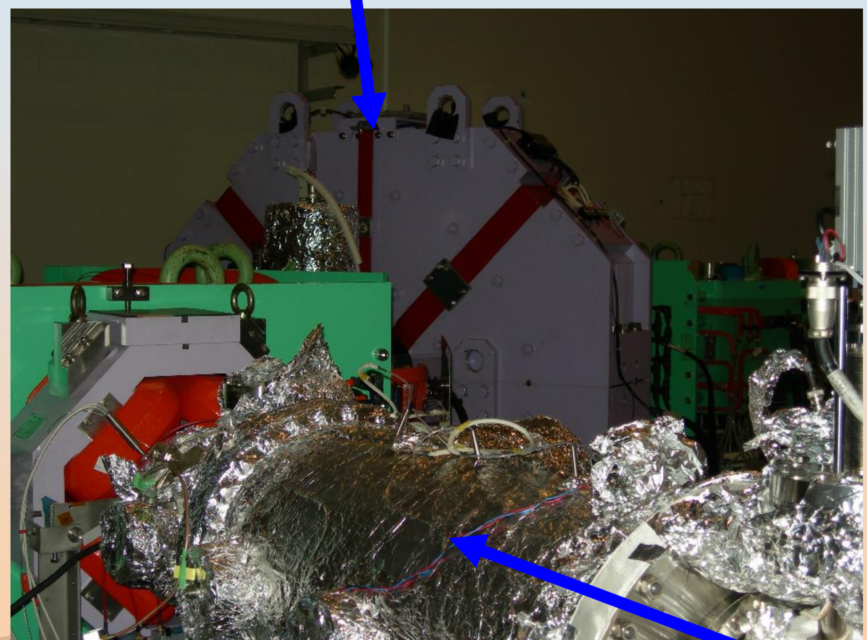

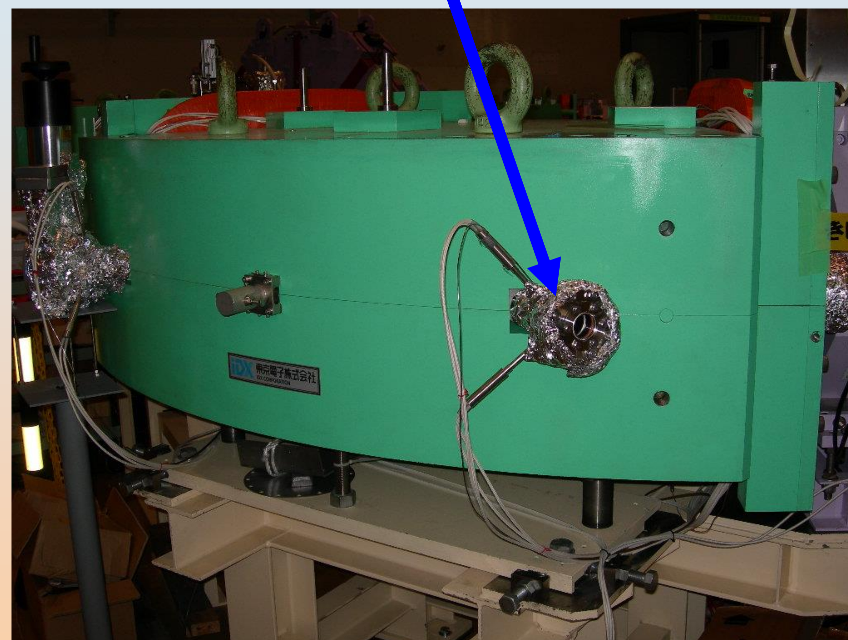

Helical Schottky Pick-up for 7 MeV proton is installed here.

Overlapping of Ion and Laser Beams

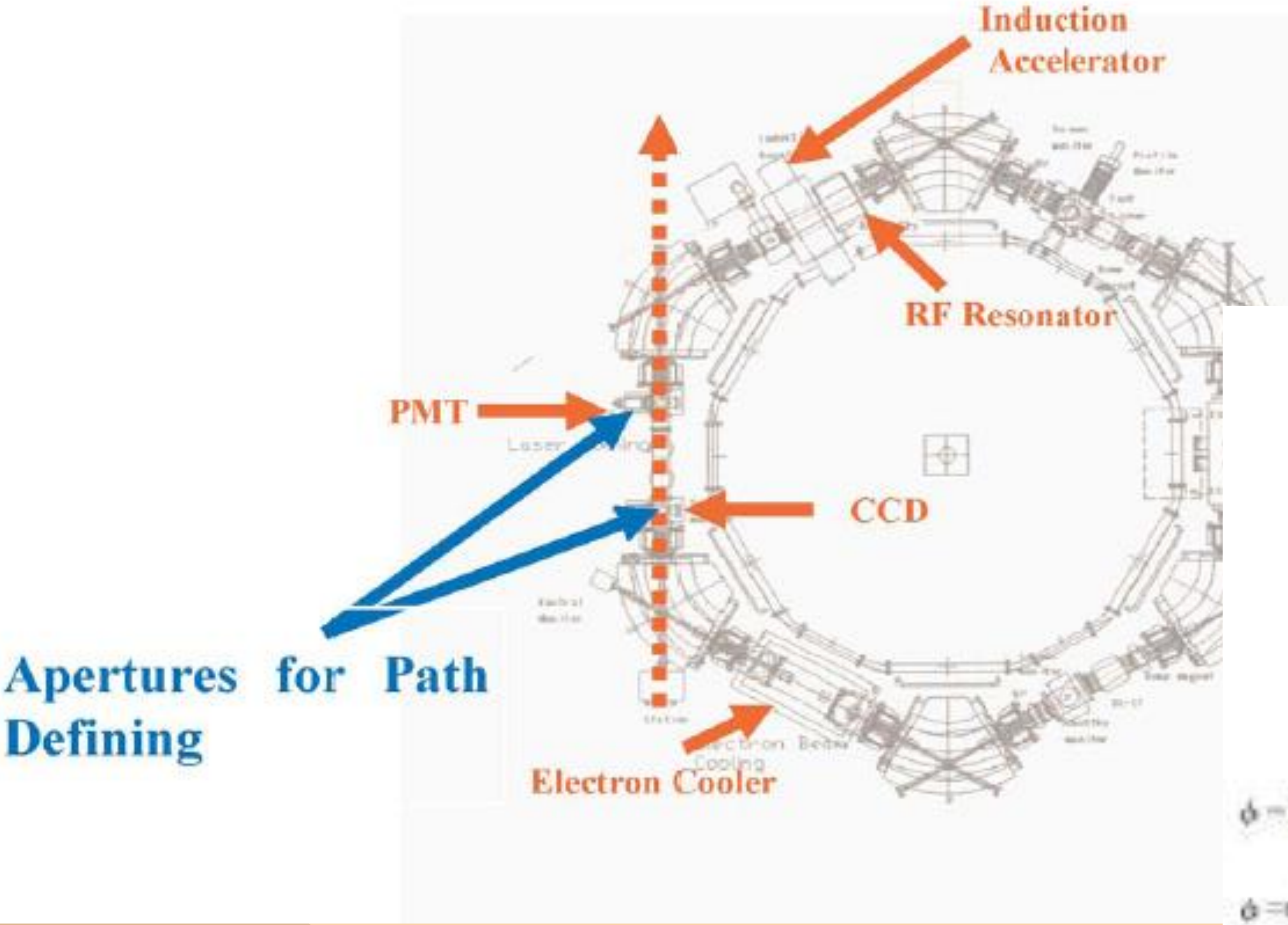

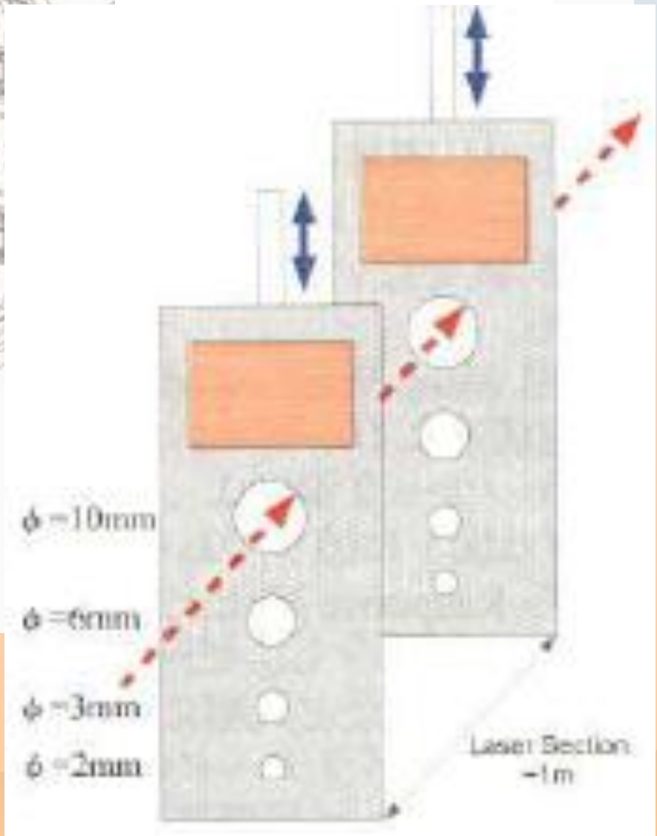

By T. Ishikawa

Post Acceleration Tube (PAT)

-Energy Sweep is applied for Distribution Measurement-

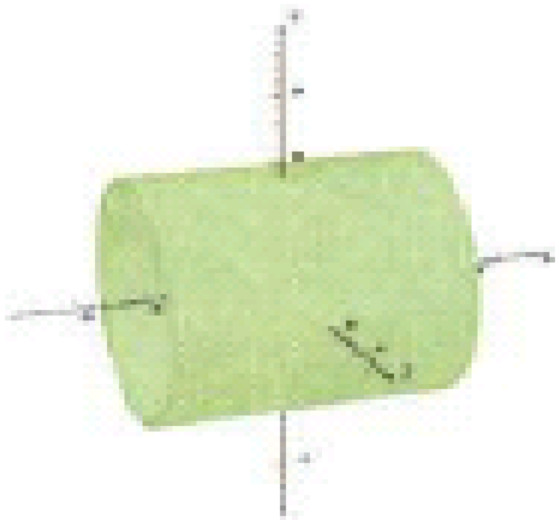

Specification of PAT

Inner Diameter	ϕ35 mm
Outer Diameter	ϕ38 mm
Length	44 mm
Observation Hole	ϕ10 mm

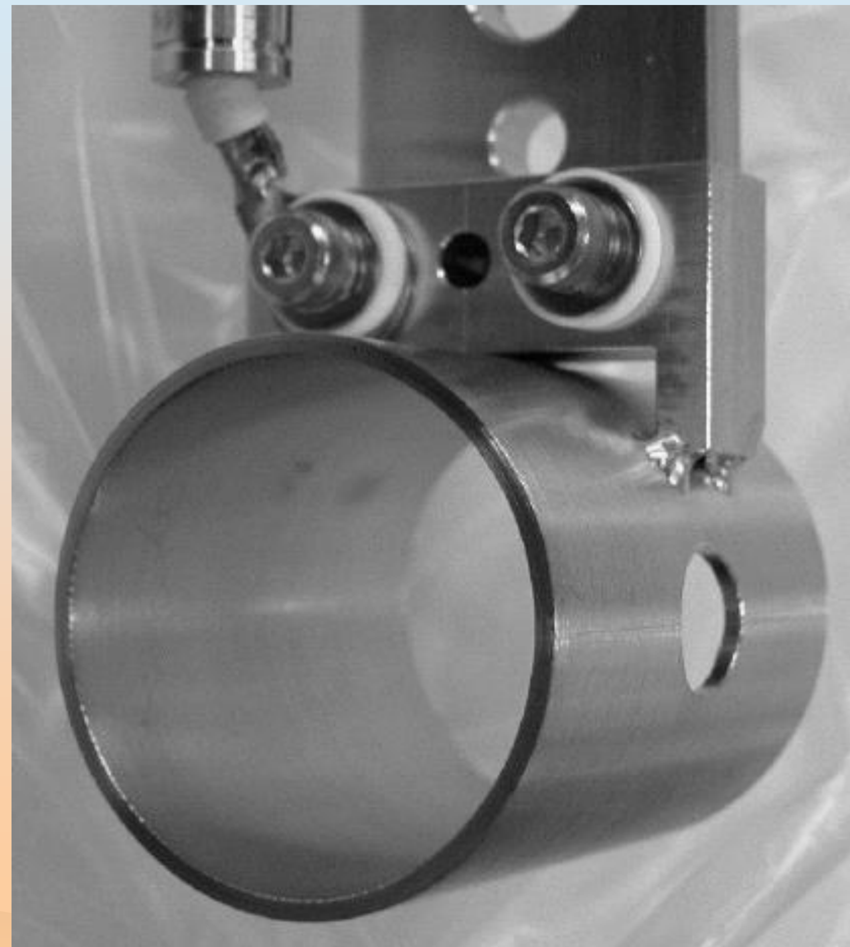

Laser Cooling of Coasting Beam at S-LSR

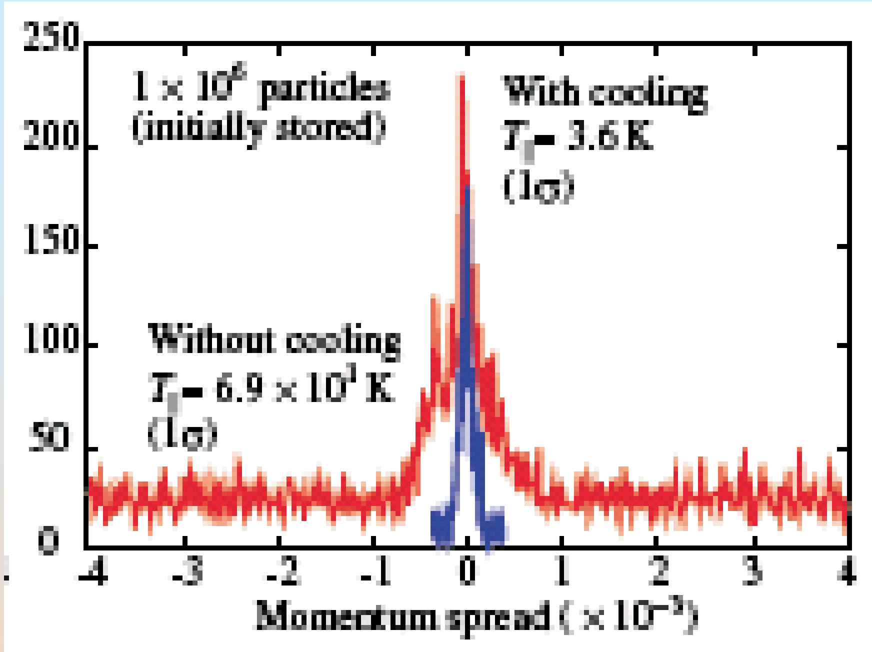

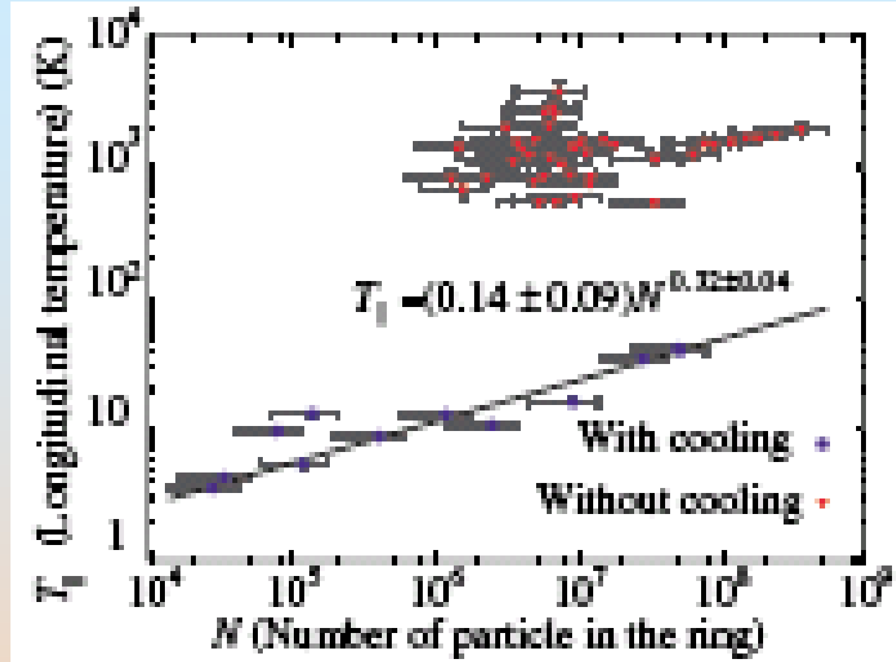

$$k_B T_\mathrm{L} = m v_0^2 \left(\frac{\Delta p}{p} \right)^2$$

$$T_L \propto N^{0.32\pm0.04}$$

$$T_L = 0.02 T_\perp$$

$$\Lambda_{IBS} \propto N \Big/ T_H T_V \sqrt{T_L} \longrightarrow T_L \propto N^{0.4}$$

Bunched Beam Cooling

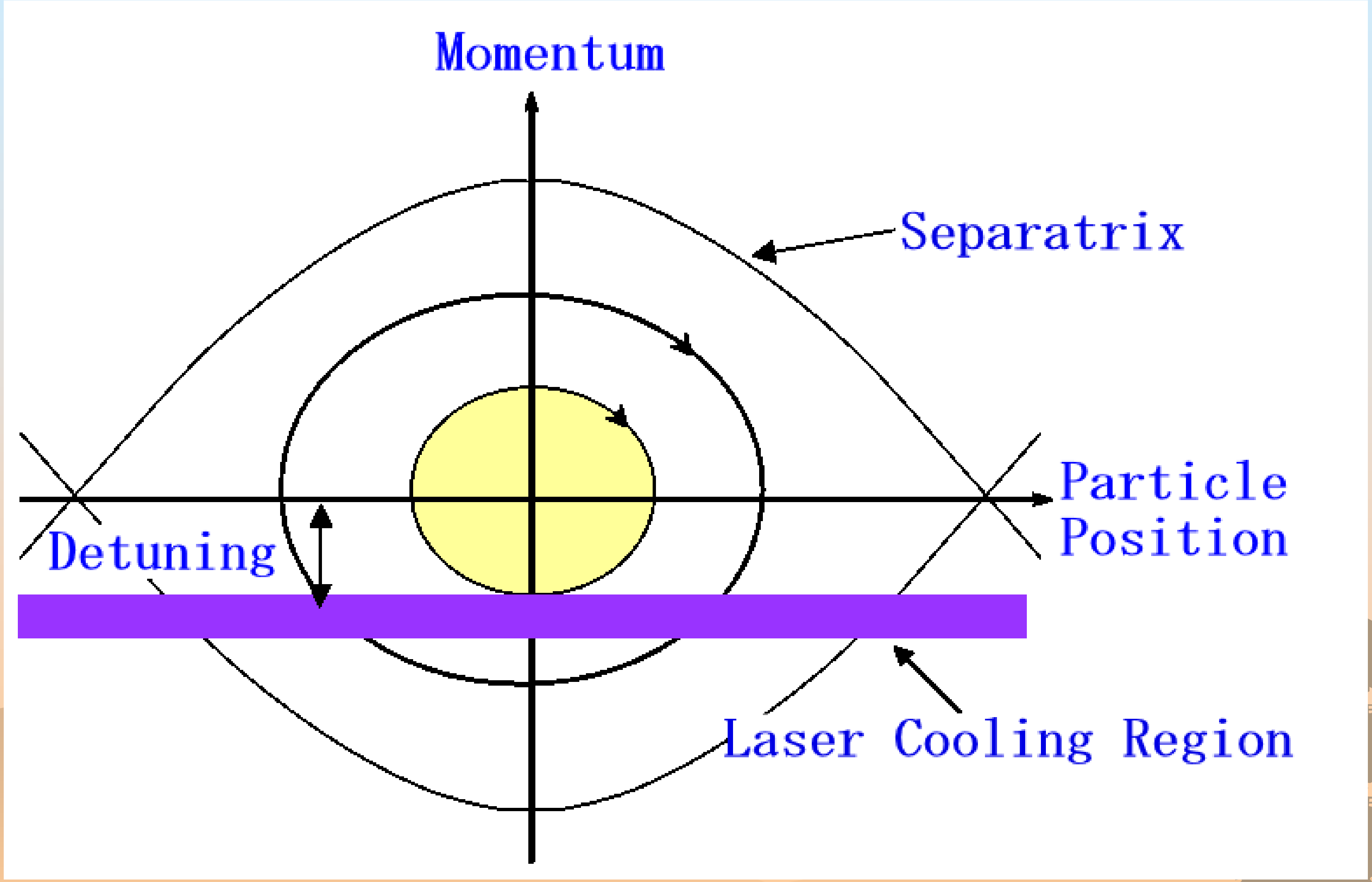

M. Nakao, Master Thesis, Kyoto University (2008)

Result of Bunched Beam Cooling

N=6x10^6 , RF Freq=125.96kHz(h=5) , Voltage=3.06V

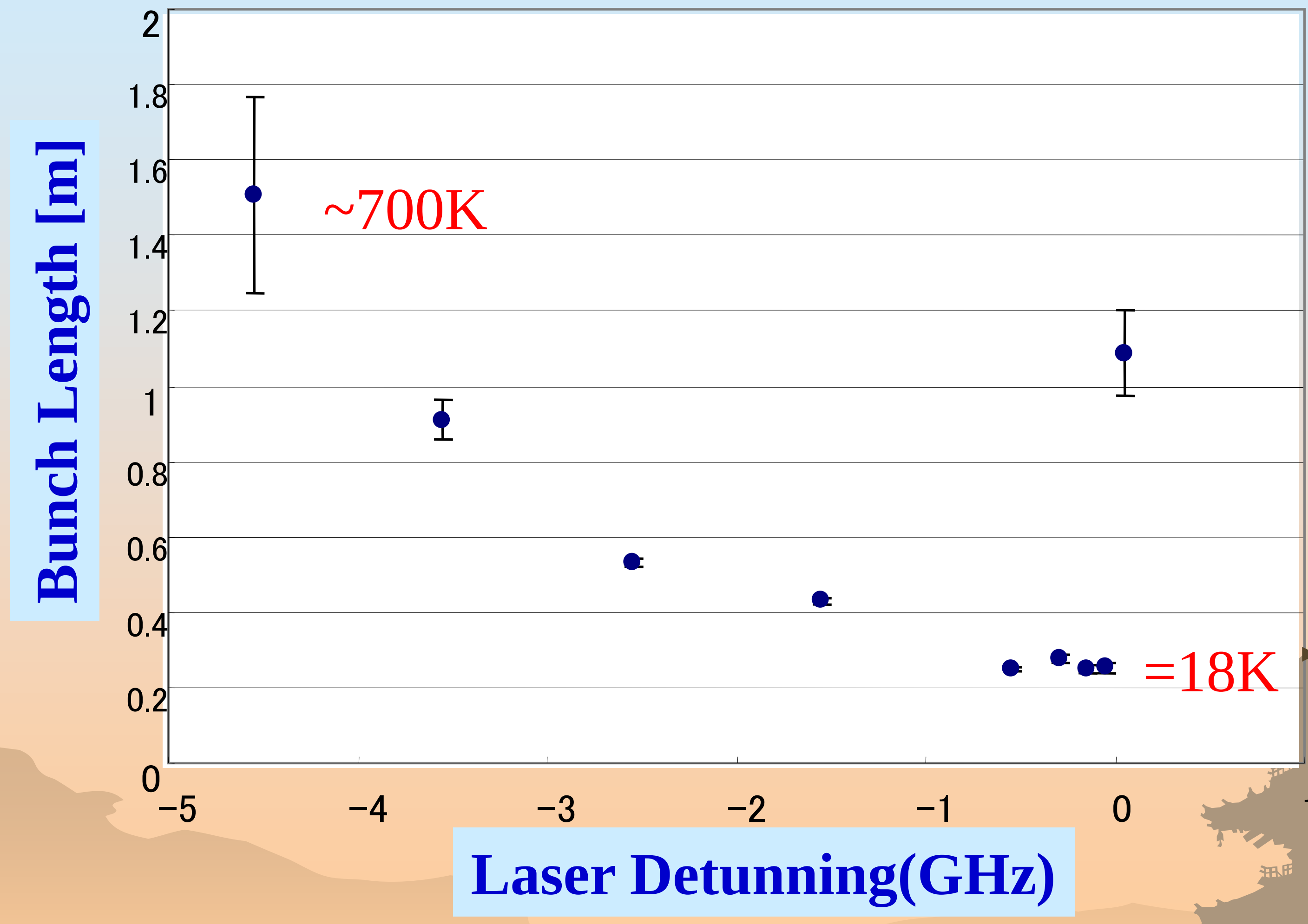

Resonant Coupling Method

―Hiromi, Andy and Dieter, Phys. Rev. Lett. 72 (1944), 3977―

$$H = \underbrace{\frac{1}{2}(p_x^2 + \kappa_x^2 x^2) + \frac{1}{2}(p_x^2 + \kappa_y^2 y^2)}_{\text{Betatron oscillation}} + \underbrace{\frac{1}{2}(p_x^2 + \kappa_z^2 z^2)}_{\text{Synchrotron oscillation (laser cooled)}} + \psi_c$$

Controllable coupling potential

- When three degrees of freedom are independent of each other ($\psi_c = 0$), nothing takes place in x and y directions even if we strongly cool the z direction.
- Switch on the coupling potential to correlate the harmonic motions in the three directions. Linear coupling potentials should be employed for this purpose:

$$\psi_c = g_1 xy \cdot \delta_p(s - s_1) + g_2 xz \cdot \delta_p(s - s_2)$$

- Move the operating point onto coupling resonance:

$$\nu_x - \nu_y = \text{integer}, \quad \nu_x - \nu_z = \text{integer}$$

Coupling Sources

- **Betatron-betatron coupling**

  Skew quadrupole magnets; Solenoid magnets, etc.

- **Synchro-betatron coupling**

  Regular RF cavities placed at dispersive positions;
  Coupling RF cavities; Wien filters, etc.

Rectangular cavity operating in a deflective mode (TM_{210}).

$$\mathbf{A} = \left(0, \quad 0, \quad g_c \cdot x \cdot \sin\omega t\right)$$

Direct vertical-longitudinal coupling can readily be generated by rotating this cavity around the axis by 90 deg.

$$H_{\mathrm{Wien}} = \frac{p_x^2 + p_y^2 + p_z^2}{2} + \frac{1}{2}\mu_x^2 x^2 - \mu_x x p_z$$

The longitudinal linear friction can naturally be tapered by a Wien filter if momentum dispersion is finite in the cooling section.

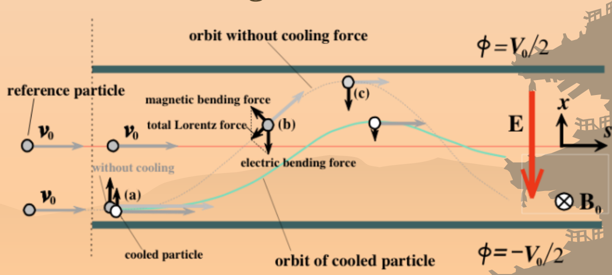

3 D Laser Cooling expected by Simulation

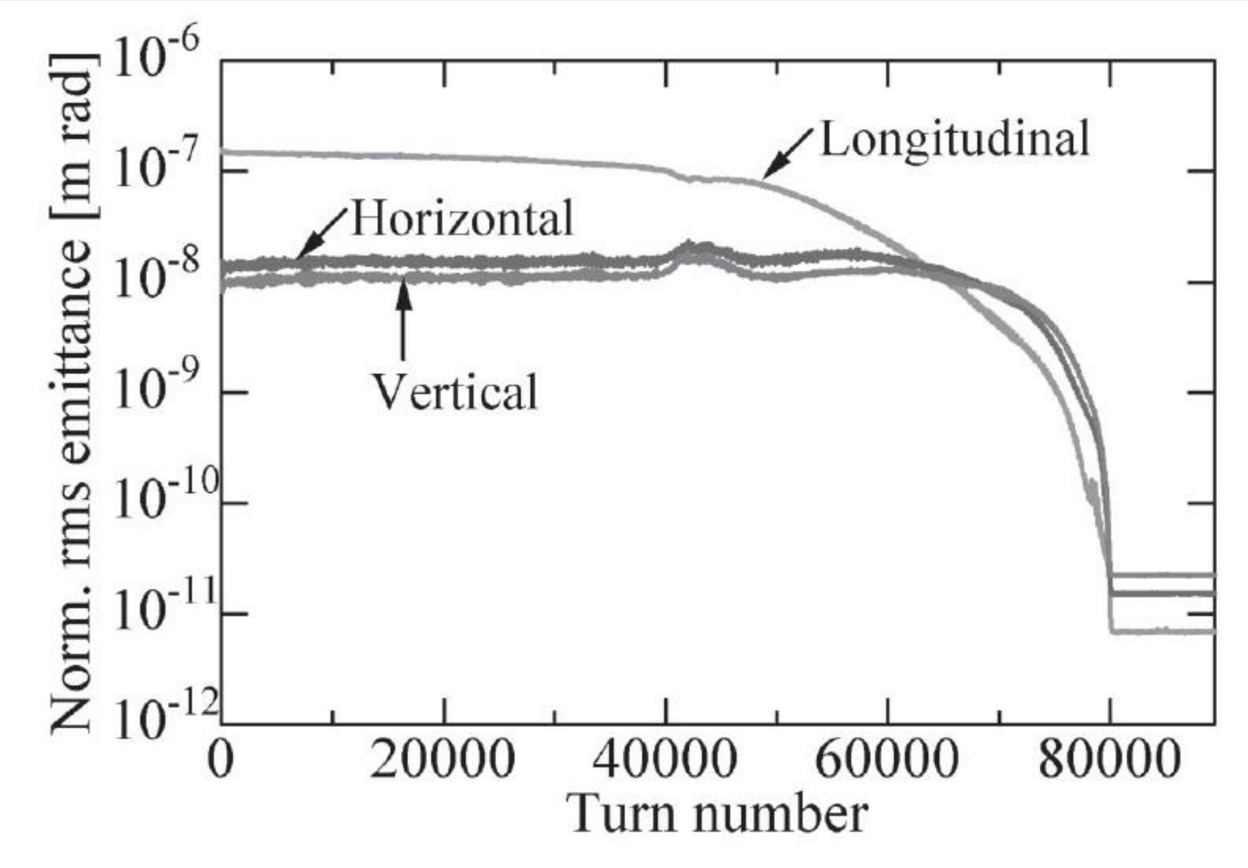

ν_H-ν_s=integer,

ν_H-ν_V=integer

Y. Yuri and H.Okamoto,
Phys. Rev. ST-AB, 8,114201 (2005)

From A. Noda et al., New Journal of Physics 8 (2006) 288

Beta- and Dispersion Functions of S-LSR

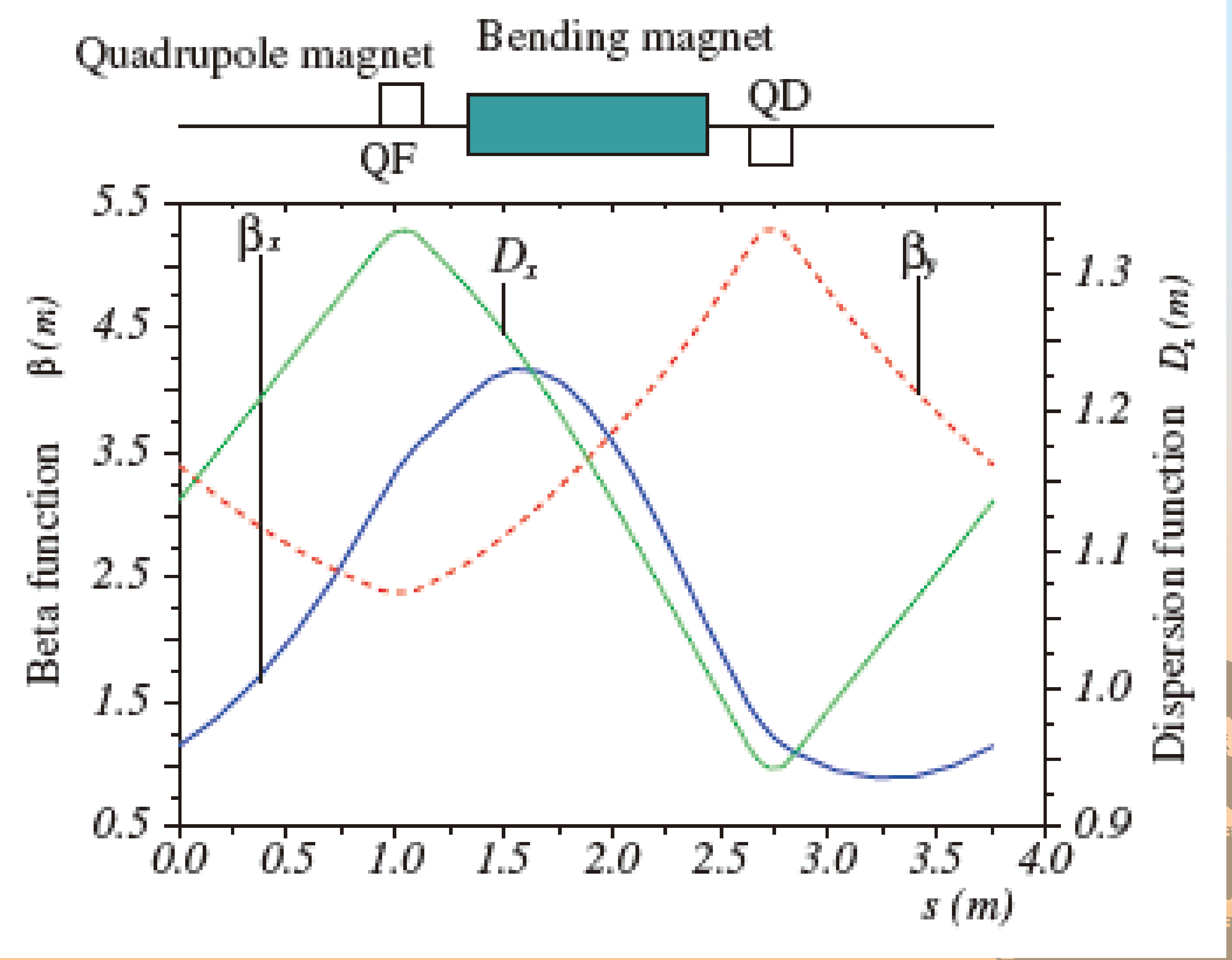

L-H Coupling

Only the relation:

ν_H-ν_s=**integer**

is satisfied!

Observation of Transverse Beam Size by CCD Camera

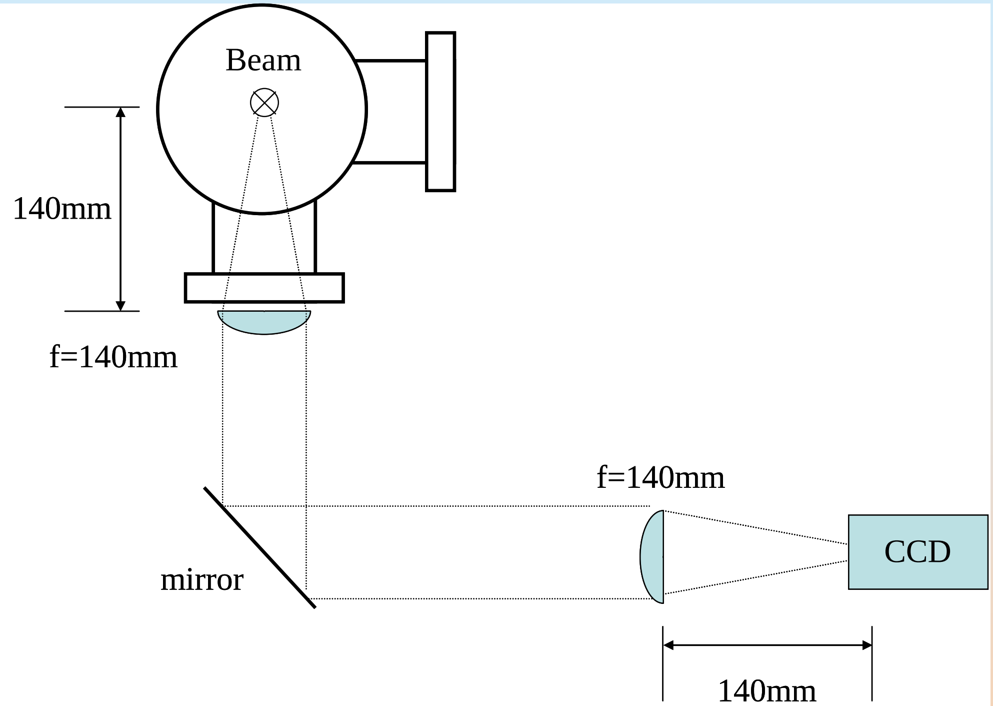

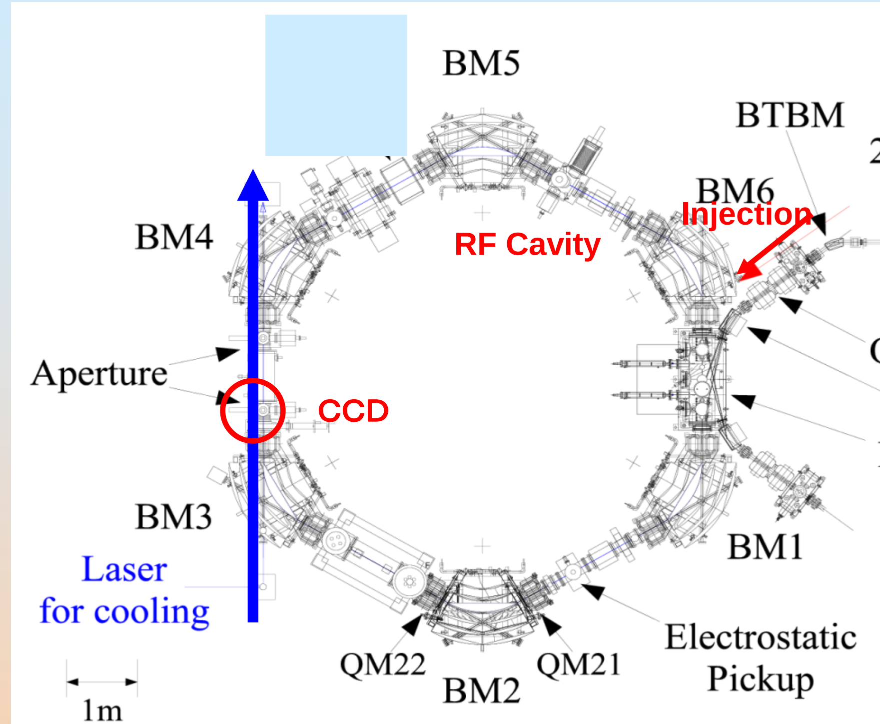

Cooled CCD Camera
(Hamamatsu Photonics C7190-11W)

Ion Observation with Emitted Light

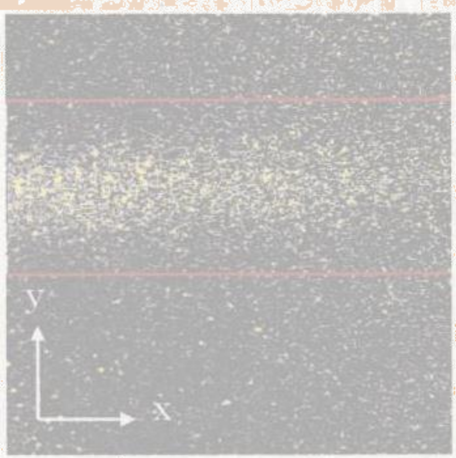

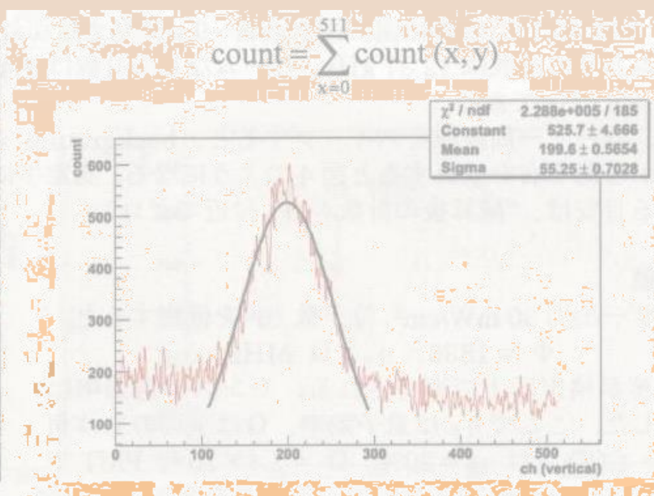

Laser Profile

Fluorescent light from the ion beam

M. Nakao et al. Phys. Rev. ST Accel. Beams 15, 110102 (2012)

Transverse Laser Cooling by Synchro-Betatron Coupling

$(\nu_H, \nu_V) = (2.068, 1.105)$

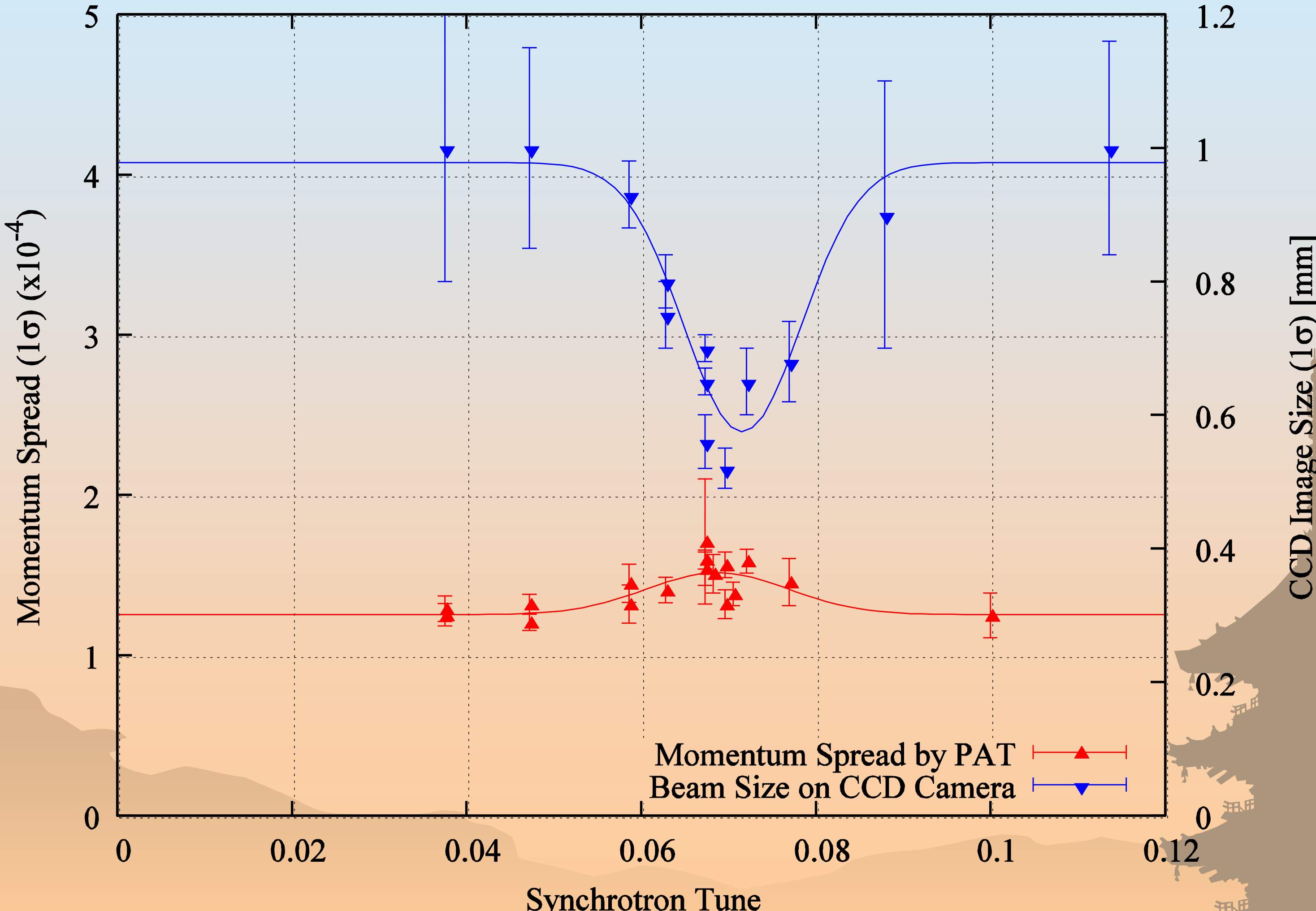

M. Nakao et al. Phys. Rev. ST Accel. Beams 15, 110102 (2012)

Time Variation of Transverse Beam Size for Various Synchrotron Tune

(Beam Intensity 1 x 10^7) **$(\nu_H, \nu_V) = (2.068, 1.105)$**

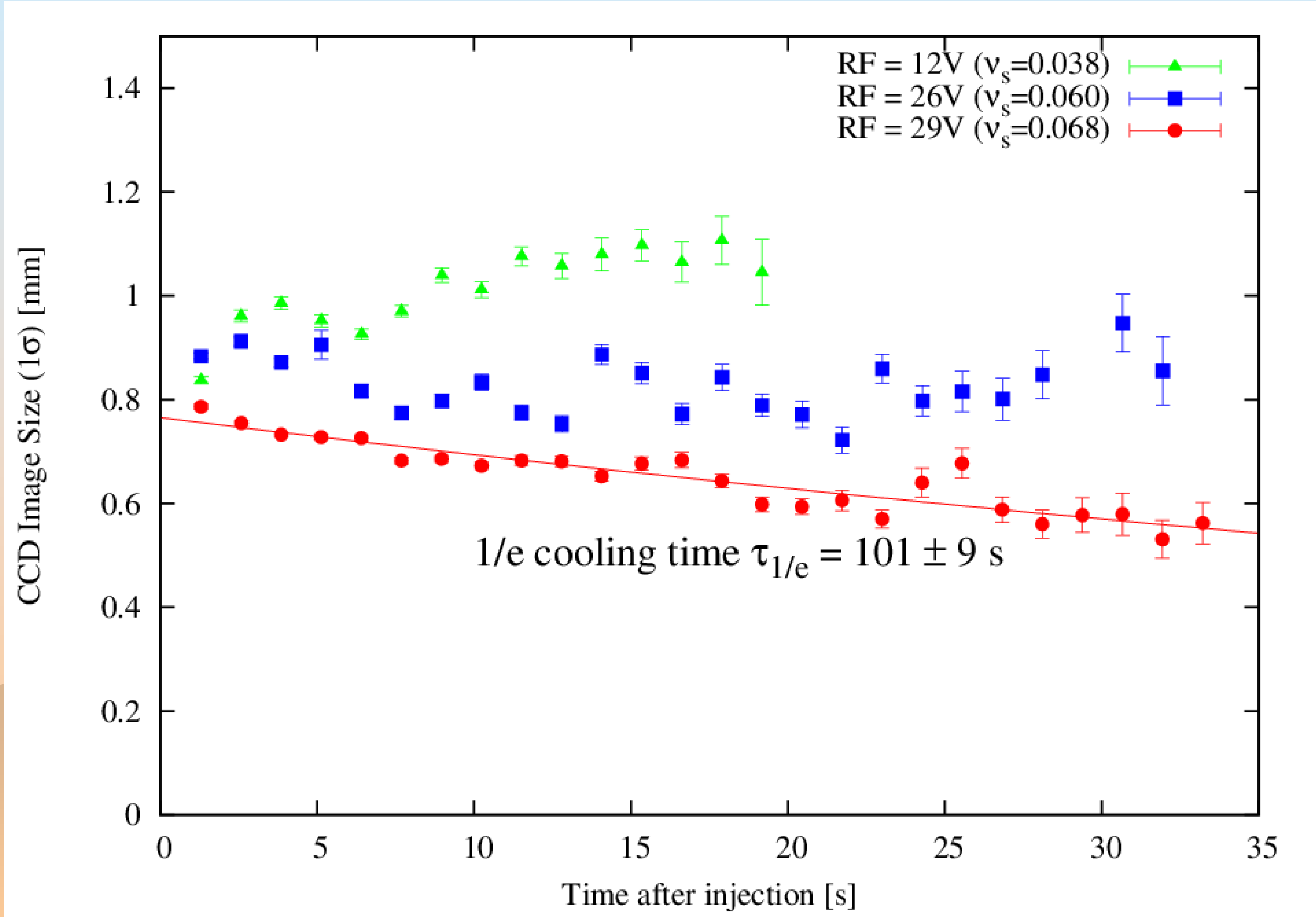

Controlled Scraping to Suppress IBS Effects

By M. Bussmann U. Schramm and D. Habs et al., SPARC07

He Zhengqi et al., to be published

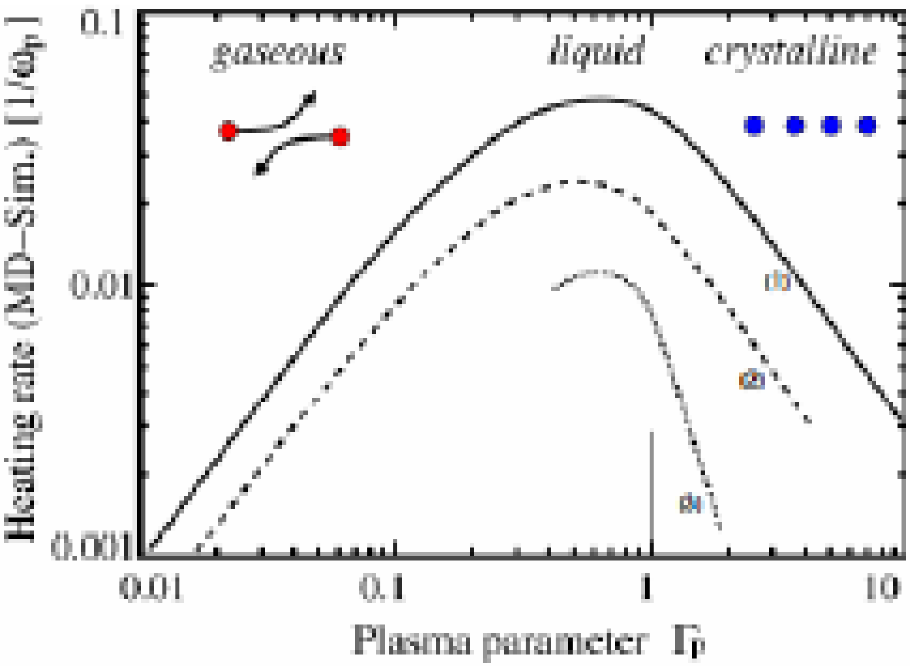

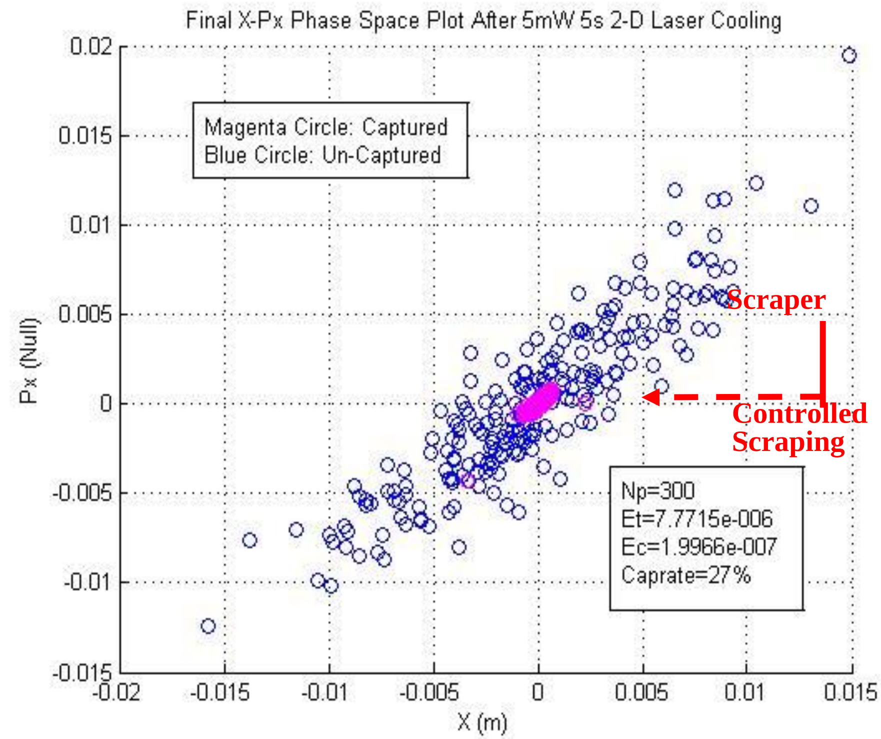

$$\Gamma_P = \frac{E_{Coulomb}}{E_{thermal}} = \frac{Z_{ion}^2 e^2}{4\pi\varepsilon_0 a_{WS} \cdot k_B T_{ion}}, \quad a_{WS} = \left(\frac{4}{3}\pi n_{ion}\right)^{-\frac{1}{3}}$$

(1): Q. Spreiter et al., NIM A 364 (1995), 239
(2): linear ion density reduced by a factor of 10
(3): string, J. Wei et al., PRL 80 (1998), 2606

Scraping System for Intensity Reduction and Beam Size Measurement

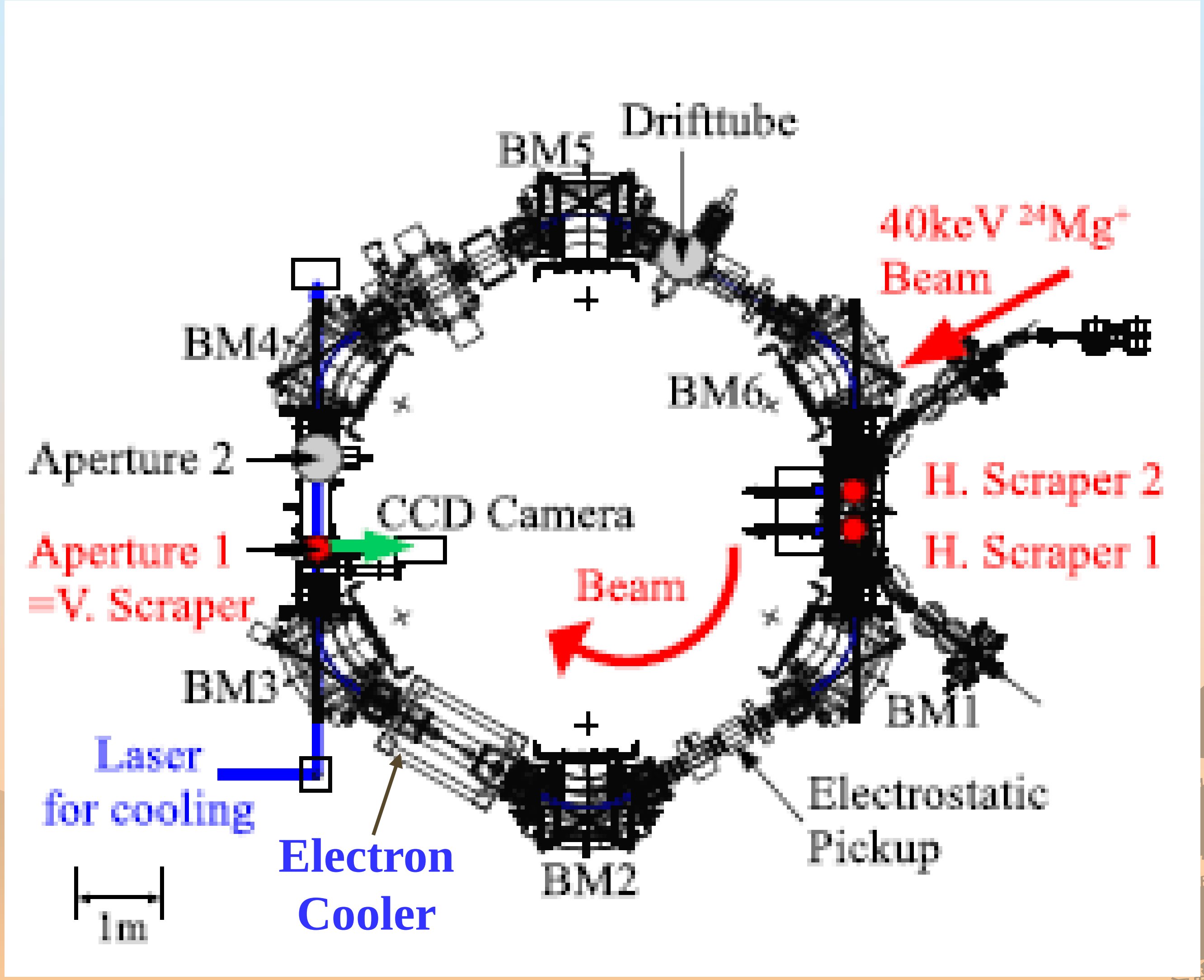

Relation between Scraper 1 Position and Surviving Beam Intensity

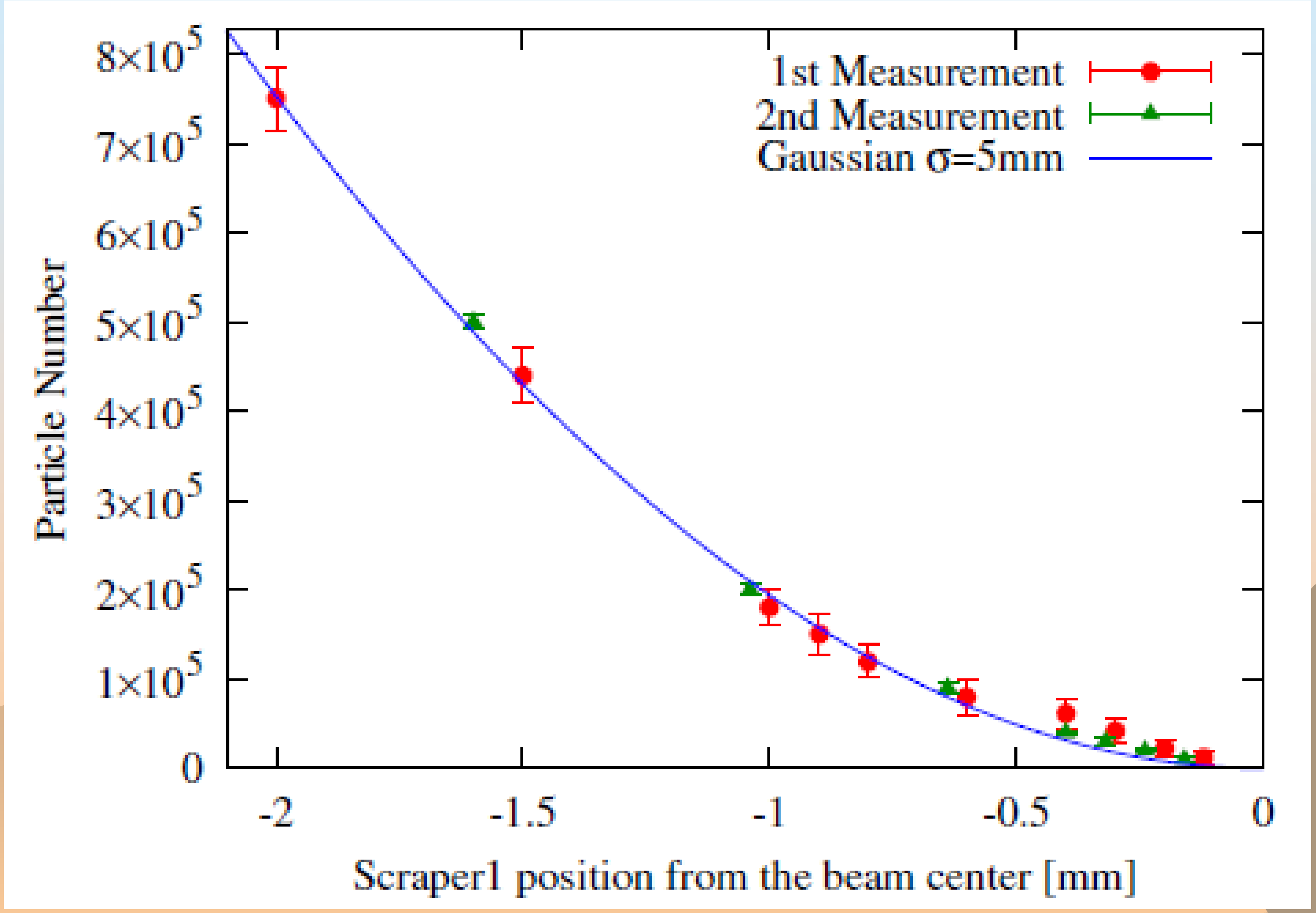

Efficiency Increase of Indirect Transverse Laser Cooling

H. Souda et al., Jpn. J. Appl. Phys. 52 (2013) 030202

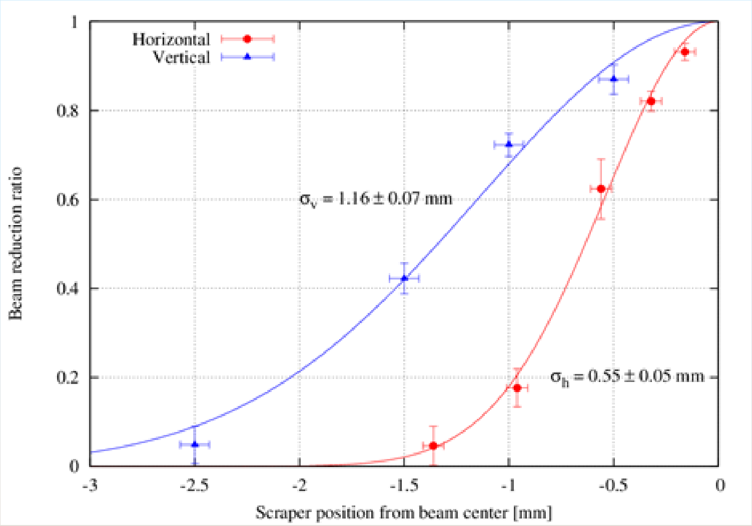

Beam size measurement by scraping

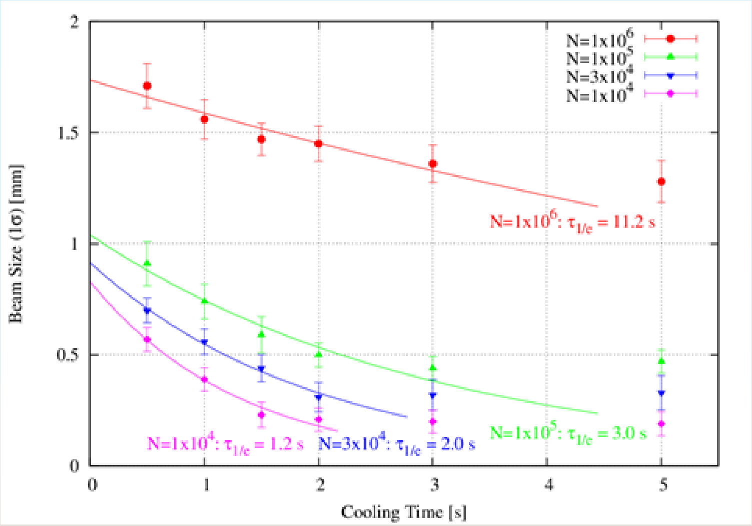

Time dependence of the cooled beam size

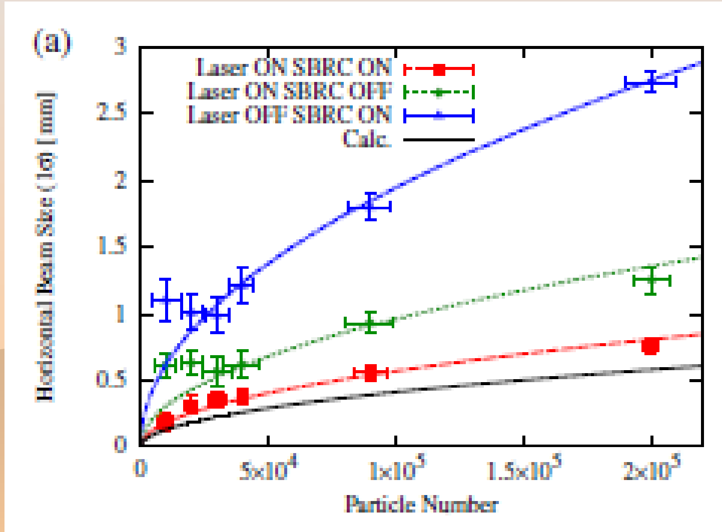

Horizontal beam size

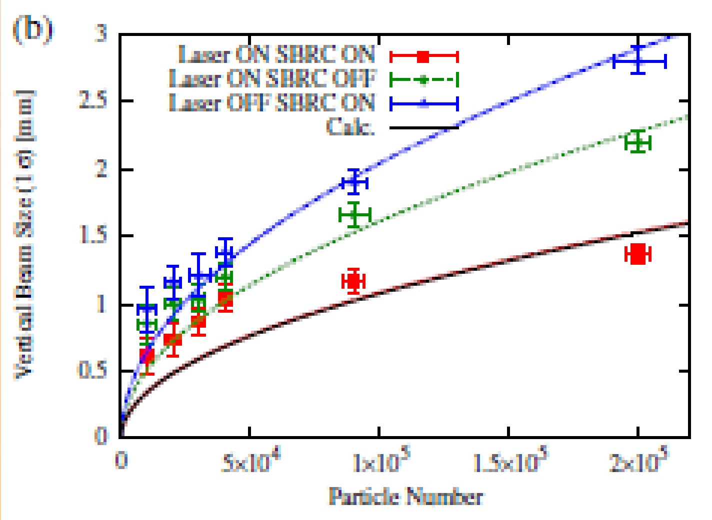

Vertical beam size

Ion Number Dependence of the Indirectly laser-cooled Laser cooled Beam Size

H-V Coupling is added

Relations:

$$\nu_H - \nu_s = \text{integer},$$

$$\nu_H - \nu_V = \text{integer}$$

are satisfied together with the use od a Solenoid

H-V Coupling with a Solenoid Field

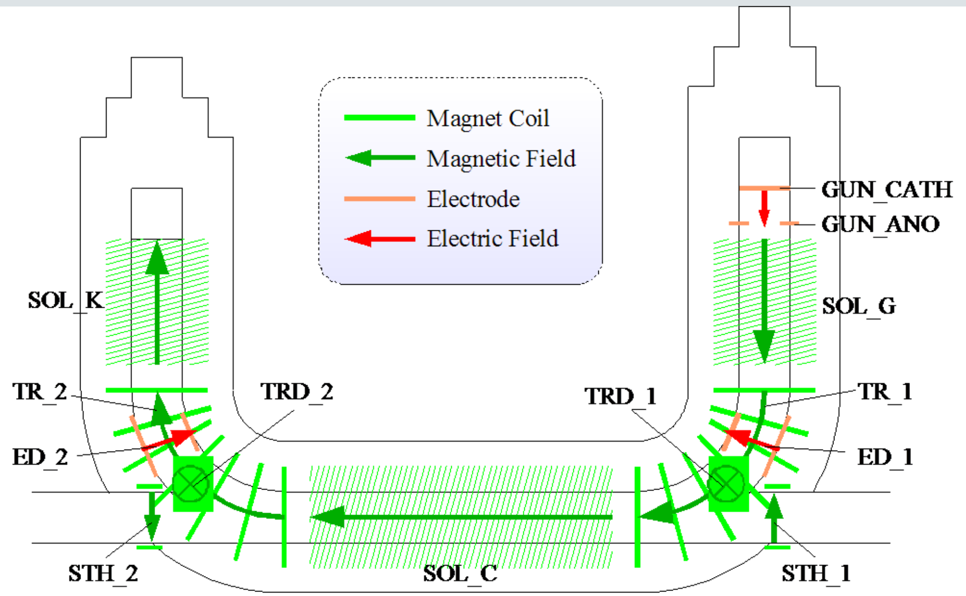

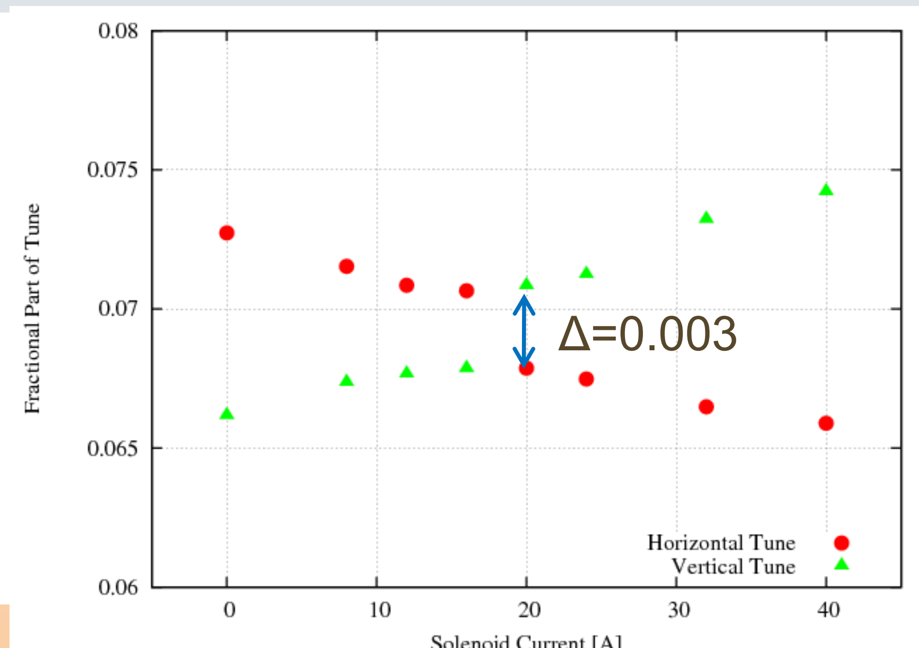

Solenoid Field of Electron Cooler (Effective Length=1.2 m)

Operating Point ~ (2.067, 1.070)

Comparison of Beam Sizes between 2D and 3D Indirect Laser Cooling

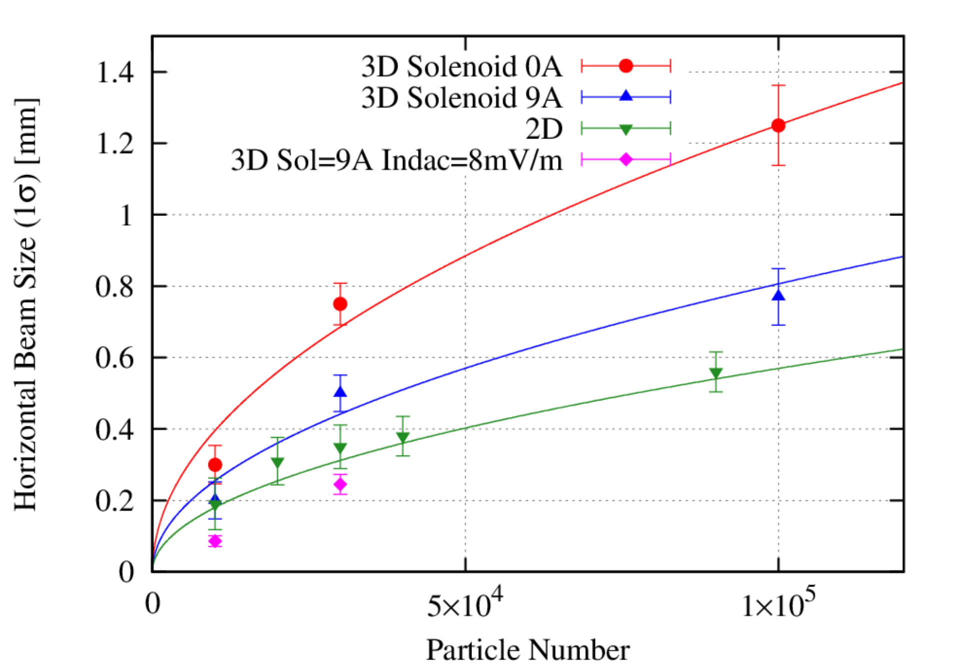

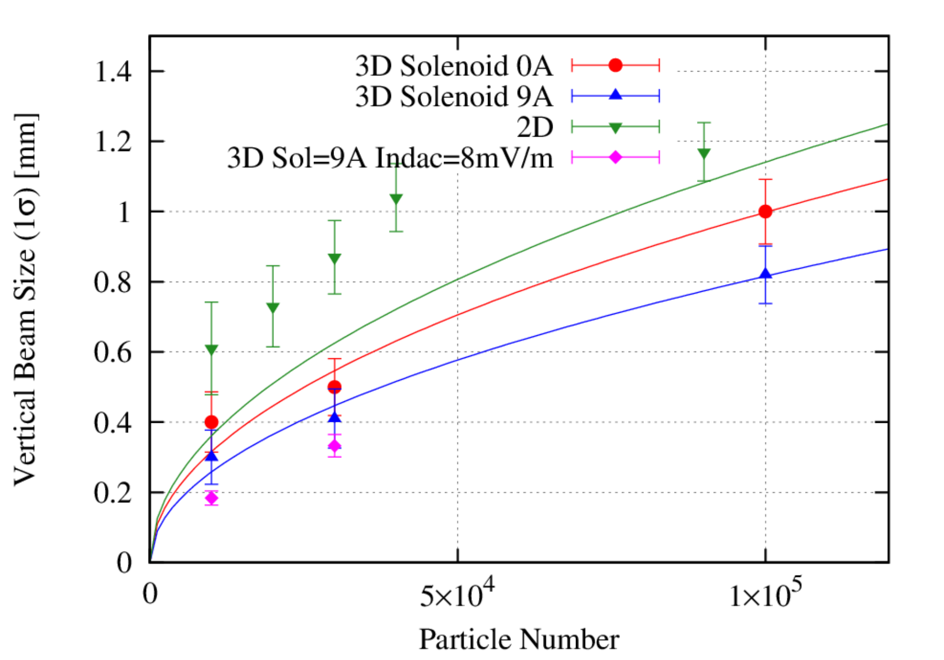

3D Laser Cooling + INDAC→Detuning Optimization

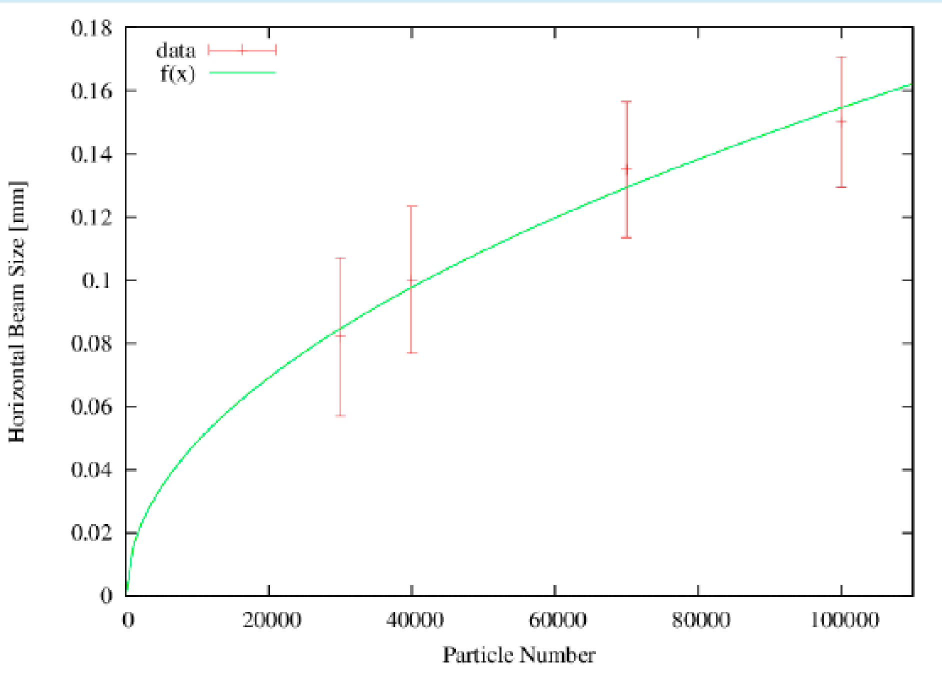

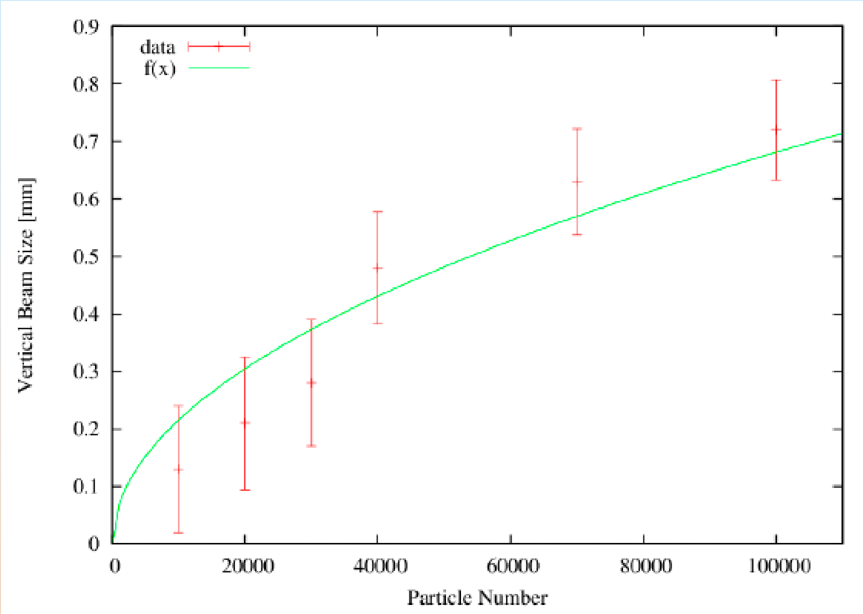

Horizontal Beam Size measured by CCD
0.08mm with the intensity of 3×10^4

Vertical Beam Size measured by a Scraper
0.13mm with the intensity of 1×10^4

$$T_y = \frac{1}{k_B} mc^2 \beta^2 \langle \gamma \rangle \frac{\sigma_y^{\ 2}}{\beta_y}$$

$$\langle \gamma \rangle = \frac{1}{C_0} \oint \frac{1+\alpha^2}{\beta} ds$$

Horizontal Beam Temperature 7.0K with 3×10^4
Vertical Beam Temperature 2.1K with 1×10^4

Comparison with Former Data

Year Ring	Method	Ion	Kinetic Energy	Intensity	$T_{//}$	T_H	T_V
1996 TSR	IBS	$^9Be^+$	7.3 MeV	2.0×10^7	15	4000	500
1998 TSR	Dispersive cooling	$^9Be^+$	7.3 MeV	1.0×10^7	few tens	~500#	~150 #
1999 ASTRID	IBS	$^{24}Mg^+$	100 keV	7×10^6	2-5	17	21
2001 PALLAS	RFQ	$^{24}Mg^+$	1 eV	1.8×10^4	<3 m	$T_\perp$<0.4	
2008 S-LSR	IBS	$^{24}Mg^+$	40 keV	1.0×10^7	11	-	500
2009 S-LSR	W SBRC (2D)	$^{24}Mg^+$	40 keV	1.0×10^7	27	220$	
2009 S-LSR	WO SBRC	$^{24}Mg^+$	40 keV	1.0×10^7	16		
2012 S-LSR	W SBRC (2D)	$^{24}Mg^+$	40 keV	1×10^4	(0.4)	20	29
2013.2.1 S-LSR	W SBRC (3D)	$^{24}Mg^+$	40 keV	1×10^4	-	40	11
2013.3.7 S-LSR (Δf=-190 MHz)	W SBRC (3D) (INDAC ON)	$^{24}Mg^+$	40 keV	1×10^4	-	8.1	4.1
2013.3.22 S-LSR (Δf=-26 MHz)	W SBRC (3D) (INDAC ON)	$^{24}Mg^+$	40 keV	1×10^4	-	7.0 (3×10^4)	2.1

Comparison between Experimental Data and Calculation

M. Grieser et al., to be published

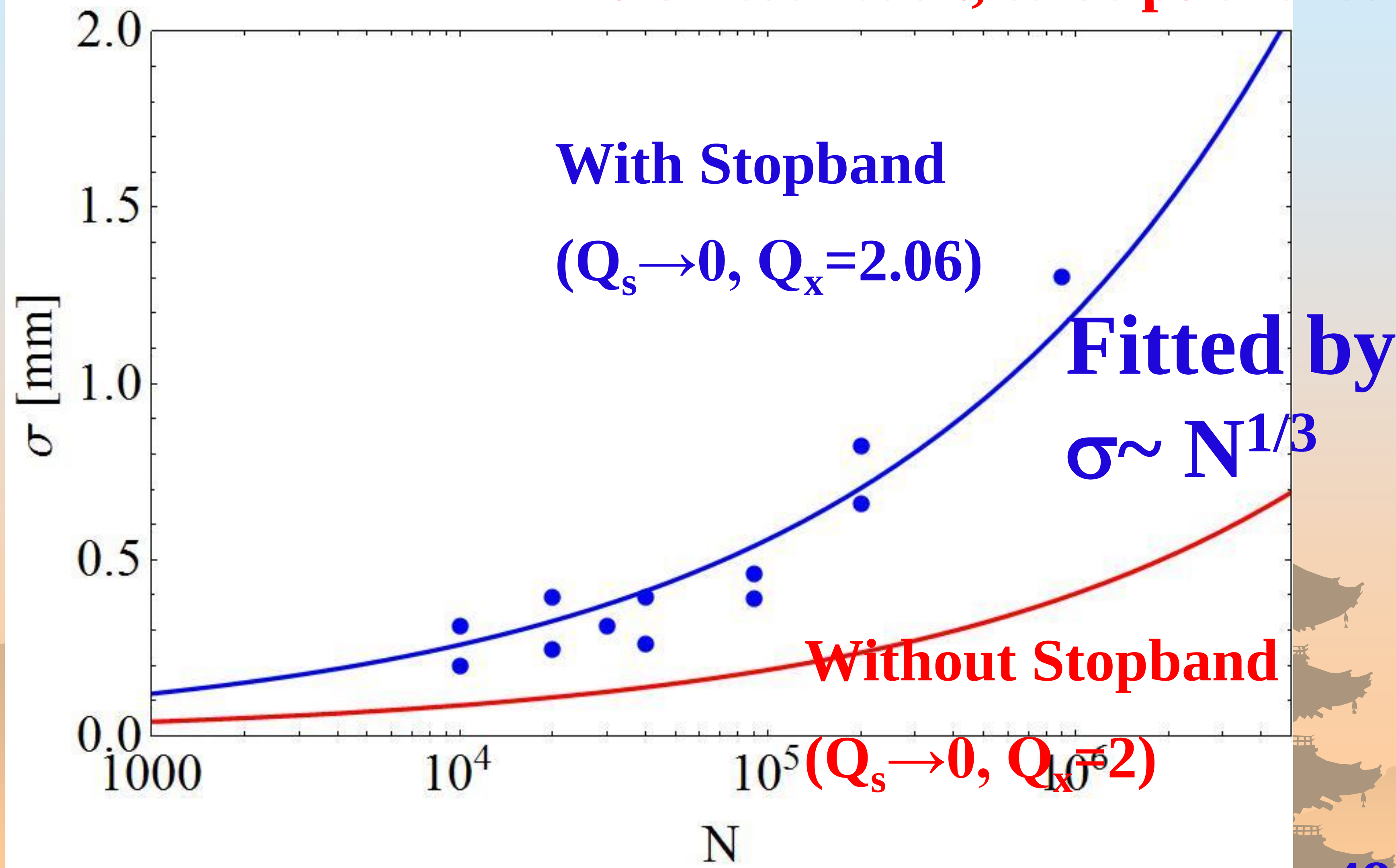

Consideration

- **Experimental Data can be well fitted by the formula $\sigma \sim N^{1/3}$ with assumption of the horizontal tune shift due to space charge stops at 2.06 due to stopband→agrees with Yuri's simulation [THAM1HA03]**
- **Trial with higher synchrotron tune to reduce the effect of stopband might realize the further reduction of the beam size.**

Present Mile Stone Attained

. Simultaneous observation of reduction of both horizontal and vertical beam sizes has been attained by laser cooling.

. IBS has been reduced by Scraping → Cooling Efficiency has been largely improved!!

- Observable down to 1 x 10^4 beam intensity
- Computer Simulation tells us that Crystal String will be expected at 10^3 beam intensity

→1 Order Improvement of Beam Observation Scheme will realize crystalline String!!

Future Perspective

Application of dispersion free lattice→3D Crystalline Beam

Shear Heating and Dispersion Suppressor

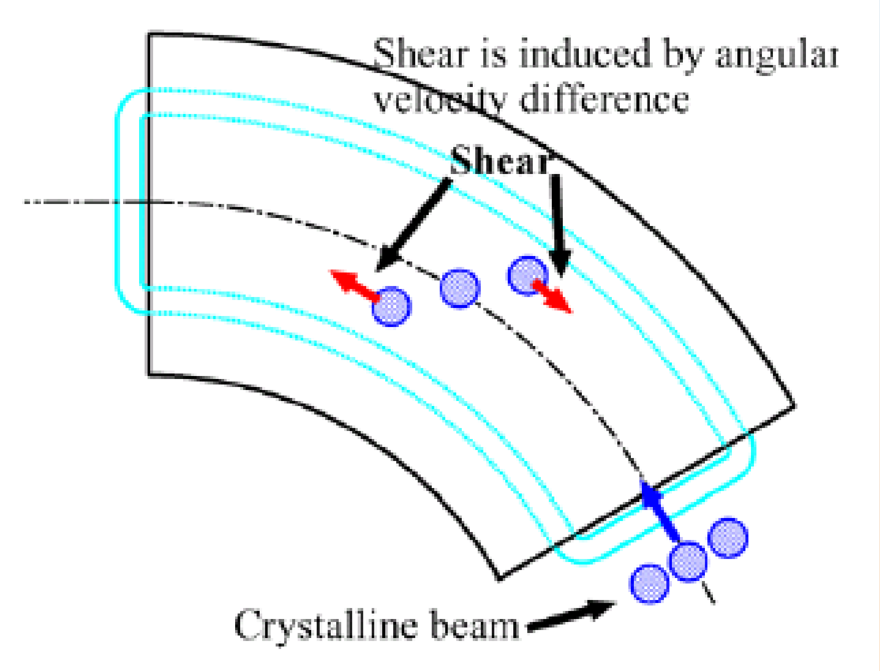

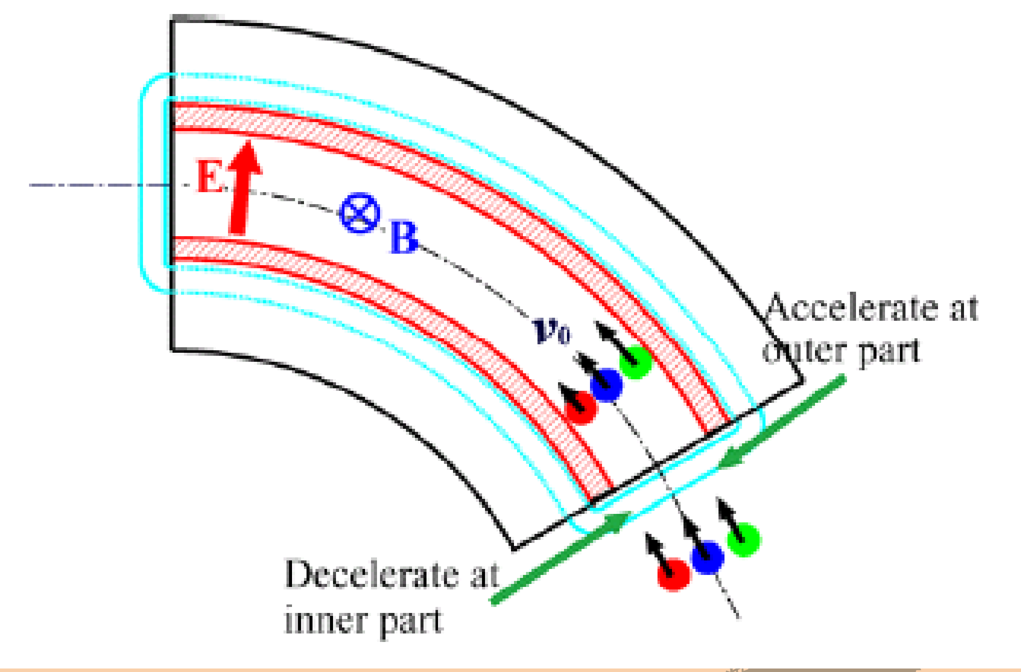

Dispersion Suppressor

$$\frac{d^2x}{ds^2}+\frac{3-n}{\rho^2}x=\frac{1}{\rho}\frac{\Delta W}{W}$$

Electric Field

$$\frac{d^2x}{ds^2}+\frac{1-n}{\rho^2}=\frac{1}{\rho}\frac{\Delta p}{p}$$

Magnetic Field

$$\frac{\Delta W}{W}=2\frac{\Delta P}{P}$$

Non-relativistic Case

$$\downarrow$$

$$2\vec{E}=-(\vec{v}\times\vec{B})$$

Acknowledgements

Heartful Thanks to all collaborators both in and outside of Japan

妻と今は亡き両親にも！

Thank you for your kind attention！

Back Up Slides

Liouville's Theorem

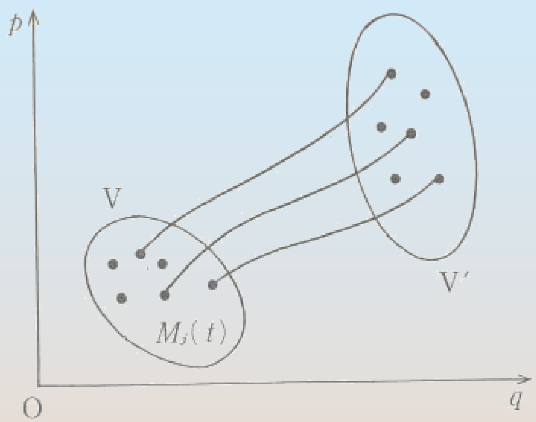

Trajectories in the 6 dimensional phase space does not cross

Laminar Flow-velocity distribution at a point which is single valued.

<u>Phase Space Density f (x,p) does not change</u>

$$\frac{df}{dt} = 0$$

Phase Space Volume occupied by the beam does not change

Beams in the accelerators basically follows Liouville's Theorem
(without inter-particle interaction)

Transverse Laser Cooling by SBRC

Heat is Transferred from Horizontal to Longitudinal Direction for this example

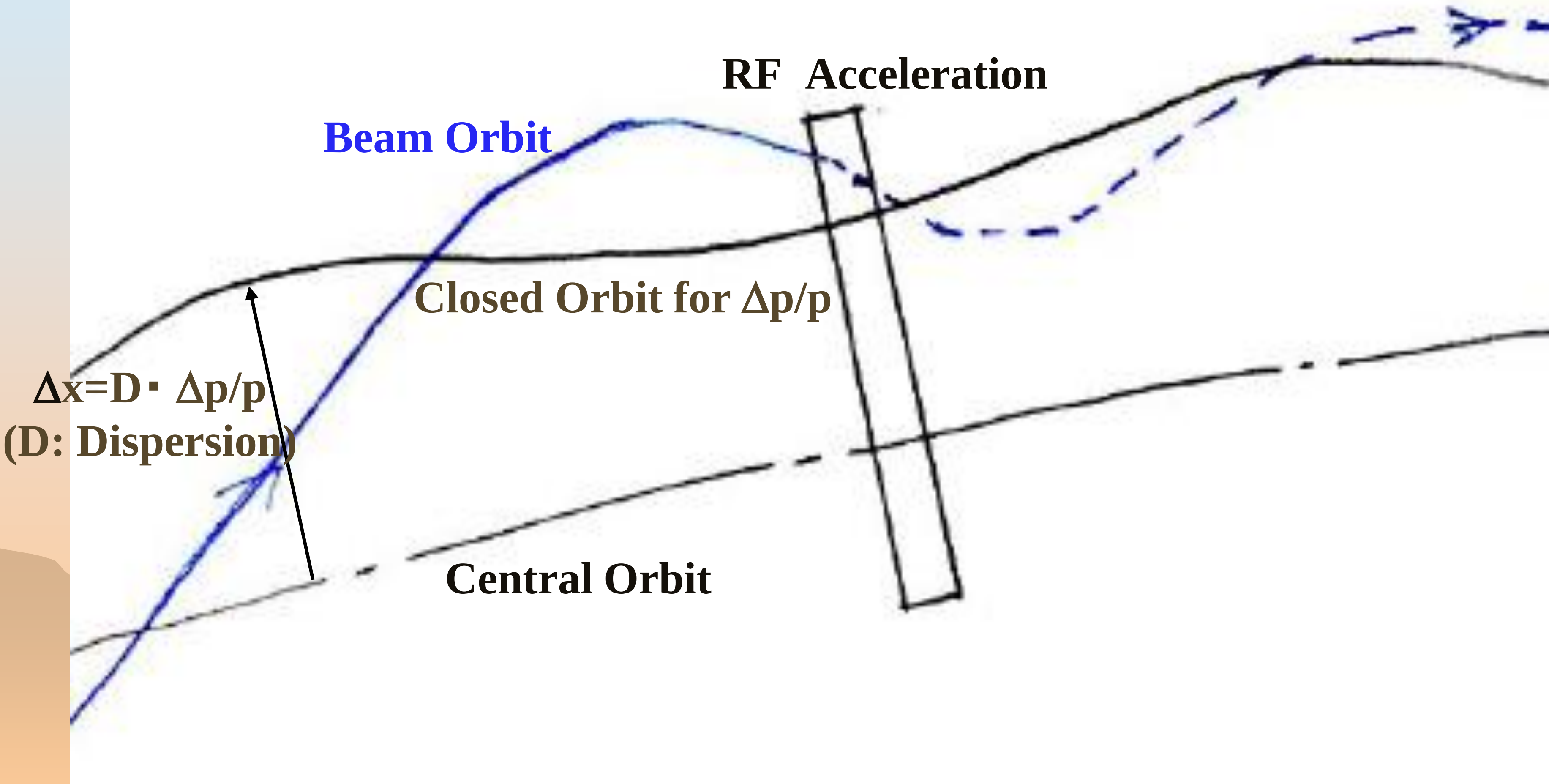

Fractional Momentum Spread vs Particle Number

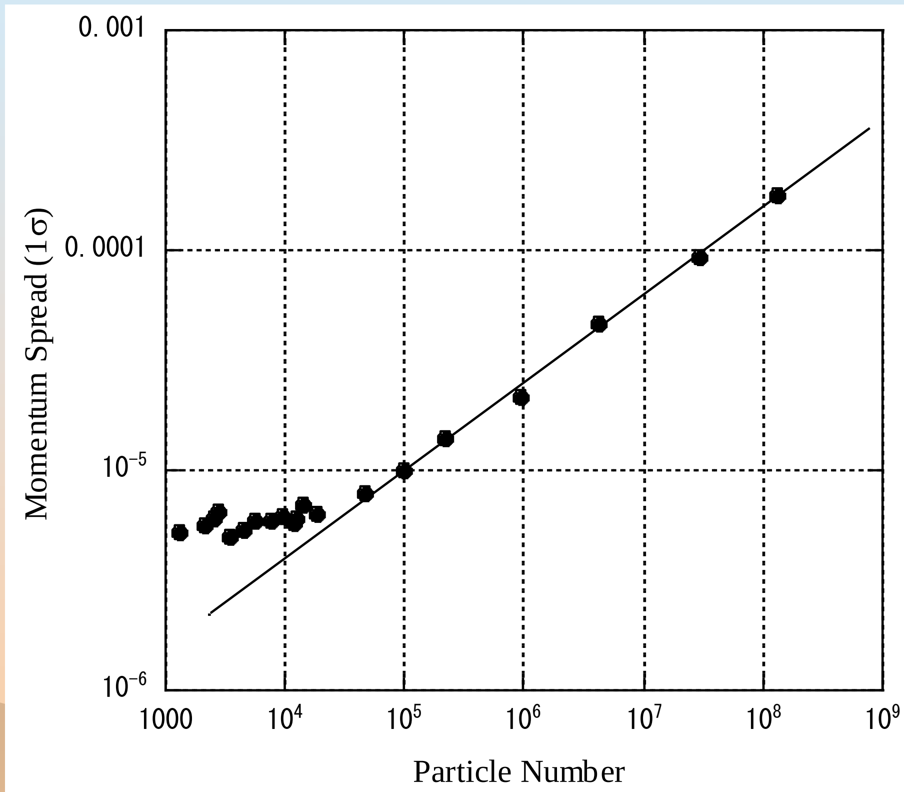

Data in Feb., 2006

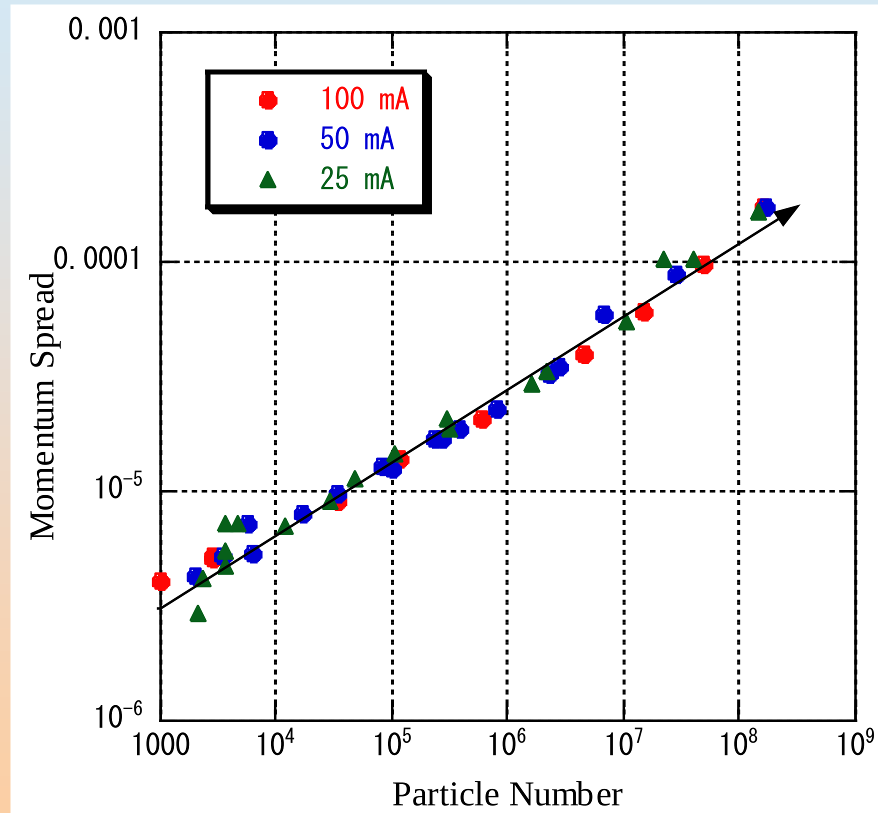

Data on the 8th, June, 2006

Reduction of Ripple in Electron Gun

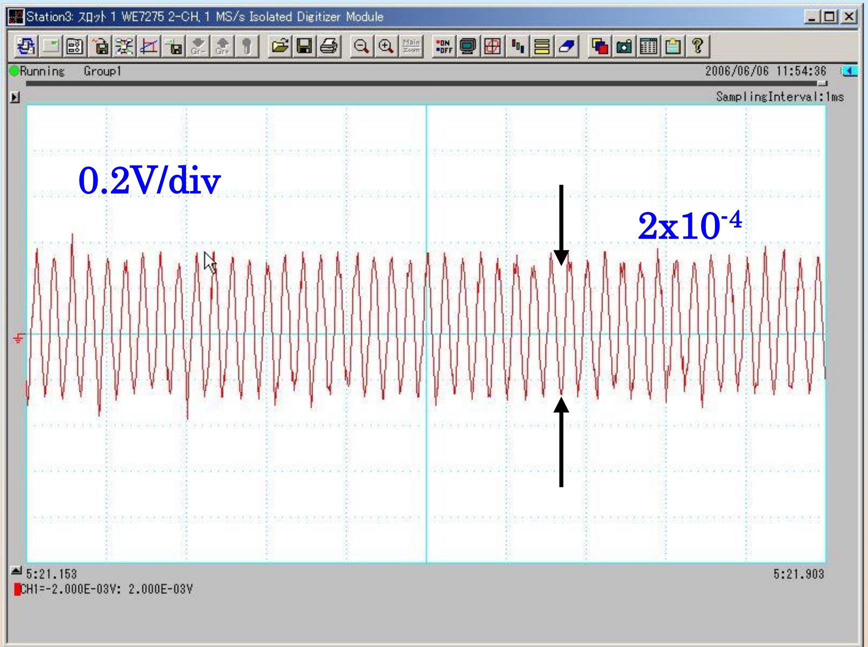

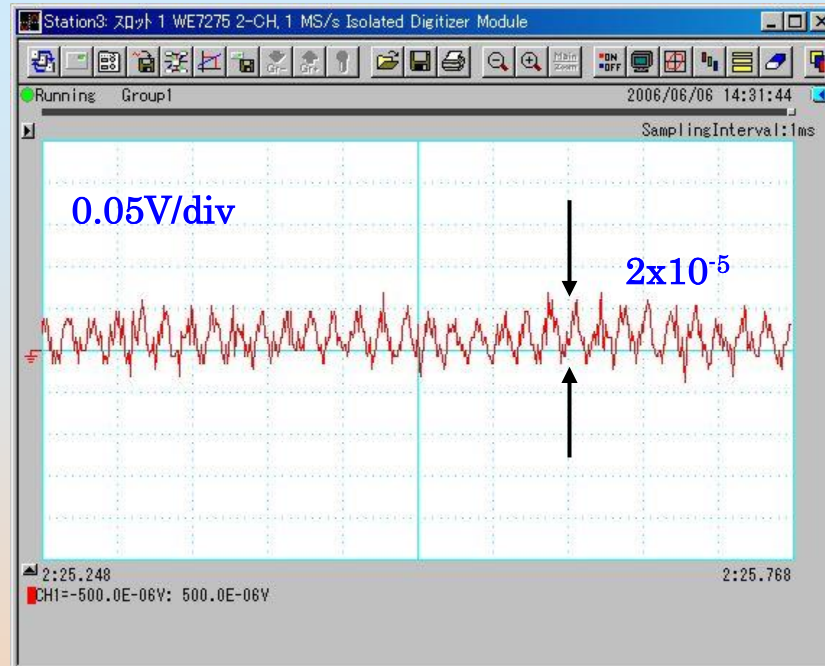

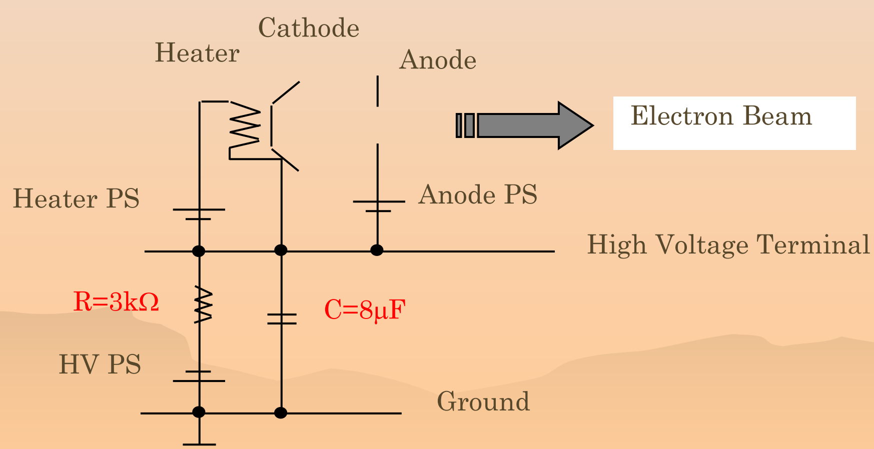

Abrupt Jump of Momentum Spread and Schottky Power

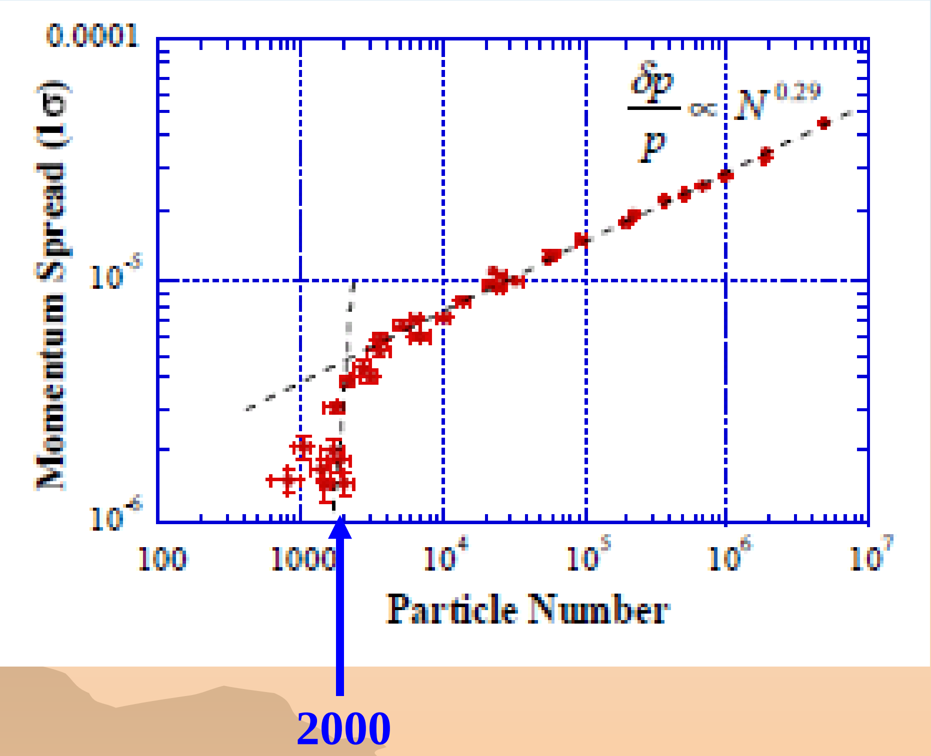

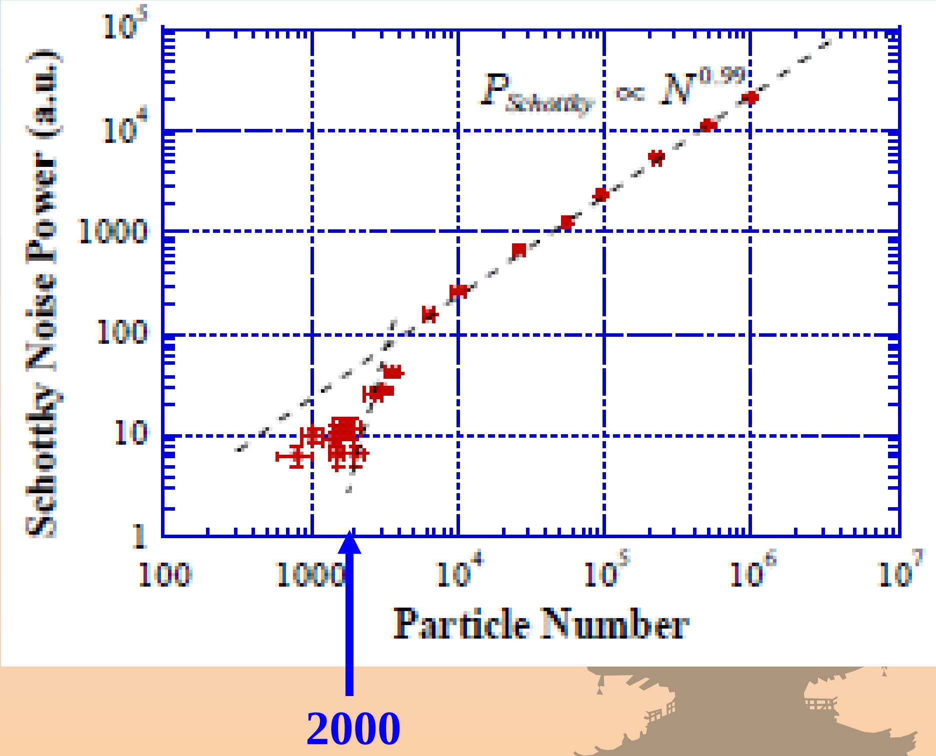

T. Shirai et al., PRL, 98 (2007) 204801

DNA Double Strand Break by Laser-produced Proton beam

A. Yogo et al., APL, 94, 181502 (2009)

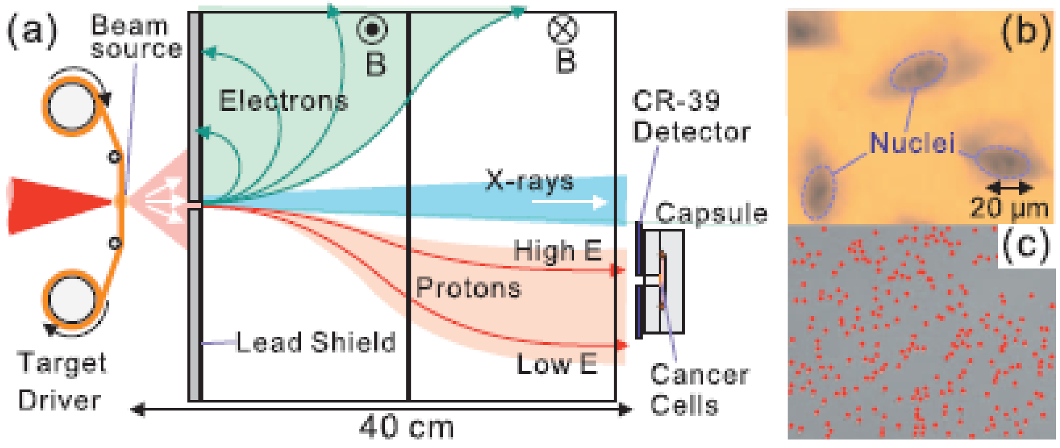

FIG. 1. (Color) (a) A schematic drawing of experimental setup. (b) An image of cancer cells taken by a microscope. (c) A spatial distribution of protons detected by CR-39 in a single laser shot. Each red point represents a single proton bombardment. The screen size is set to be same as that in the frame (b).

Pulse Width 15ns, 20 Gy

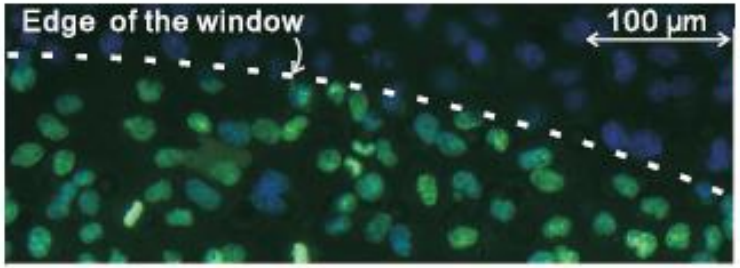

FIG. 3. (Color) γ-H2AX focus formation induced by irradiation of laser-accelerated protons with 20 Gy. γ-H2AX and nucleus are stained with anti-γ-H2AX antibody (green) and DAPI (blue).

Fast Extraction System at S-LSR

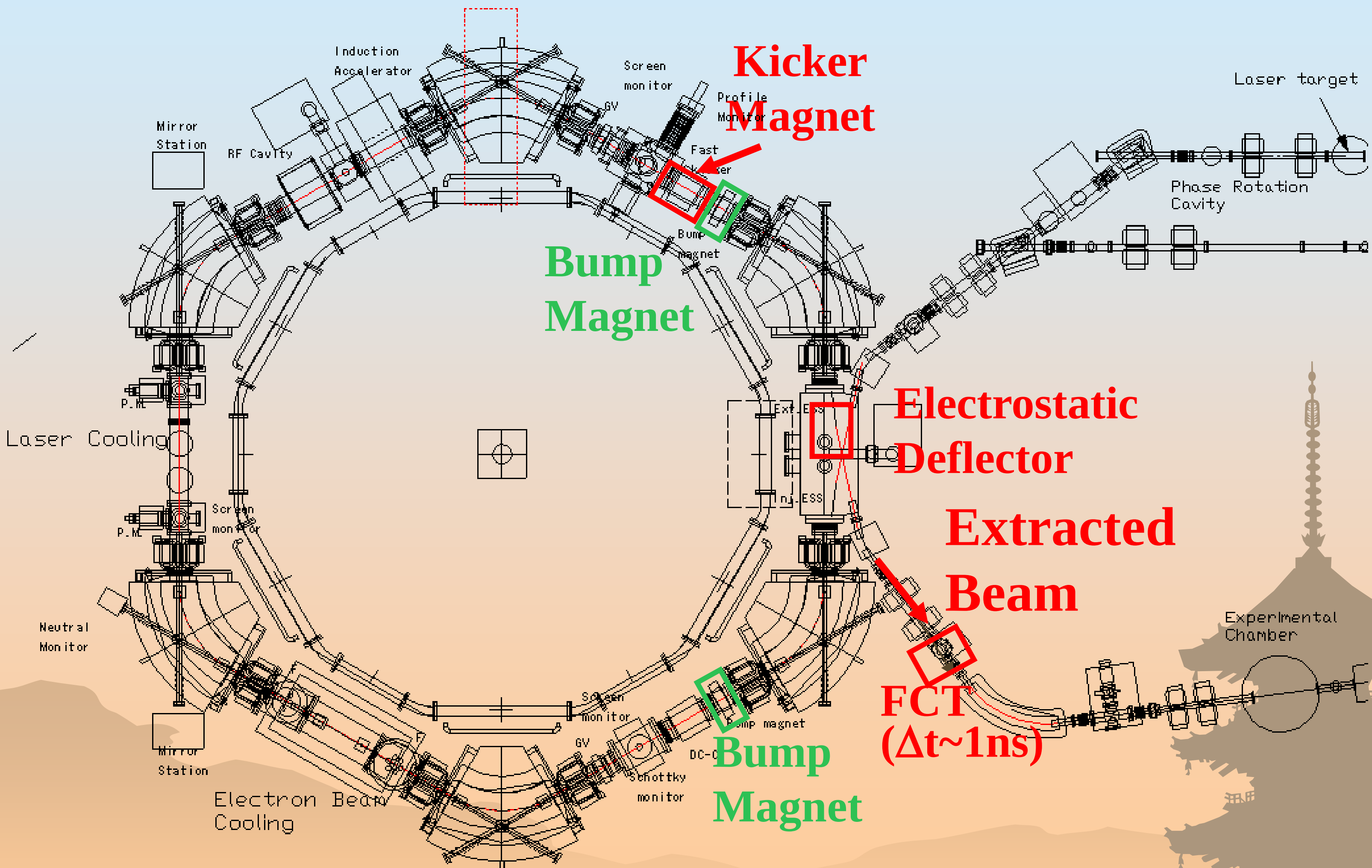

Bunch Rotation of 7 MeV Proton

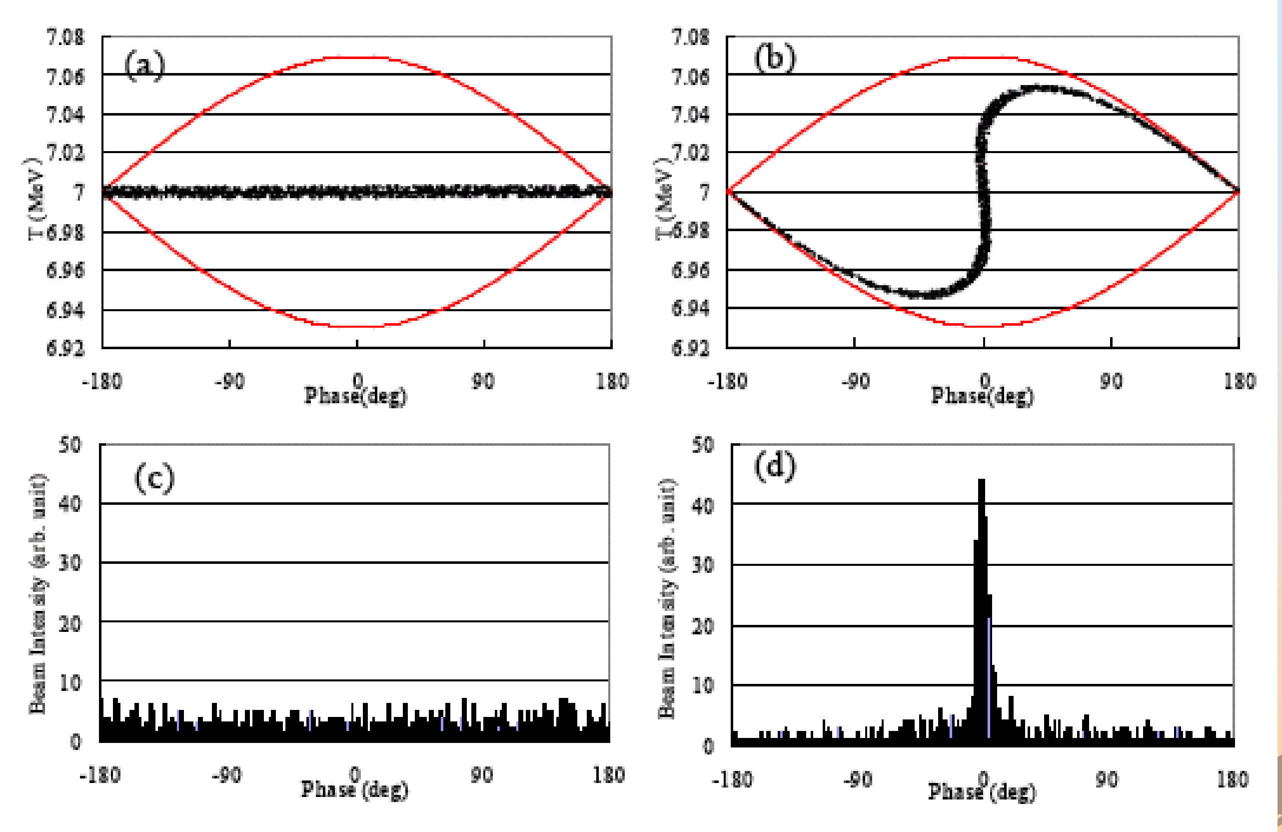

RF field (800 V) is applied to coasting beam after electron cooling and is extracted when the beam is rotated ~90°.

Vacuum Chamber in the Magnet Section (includes the Electrodes)

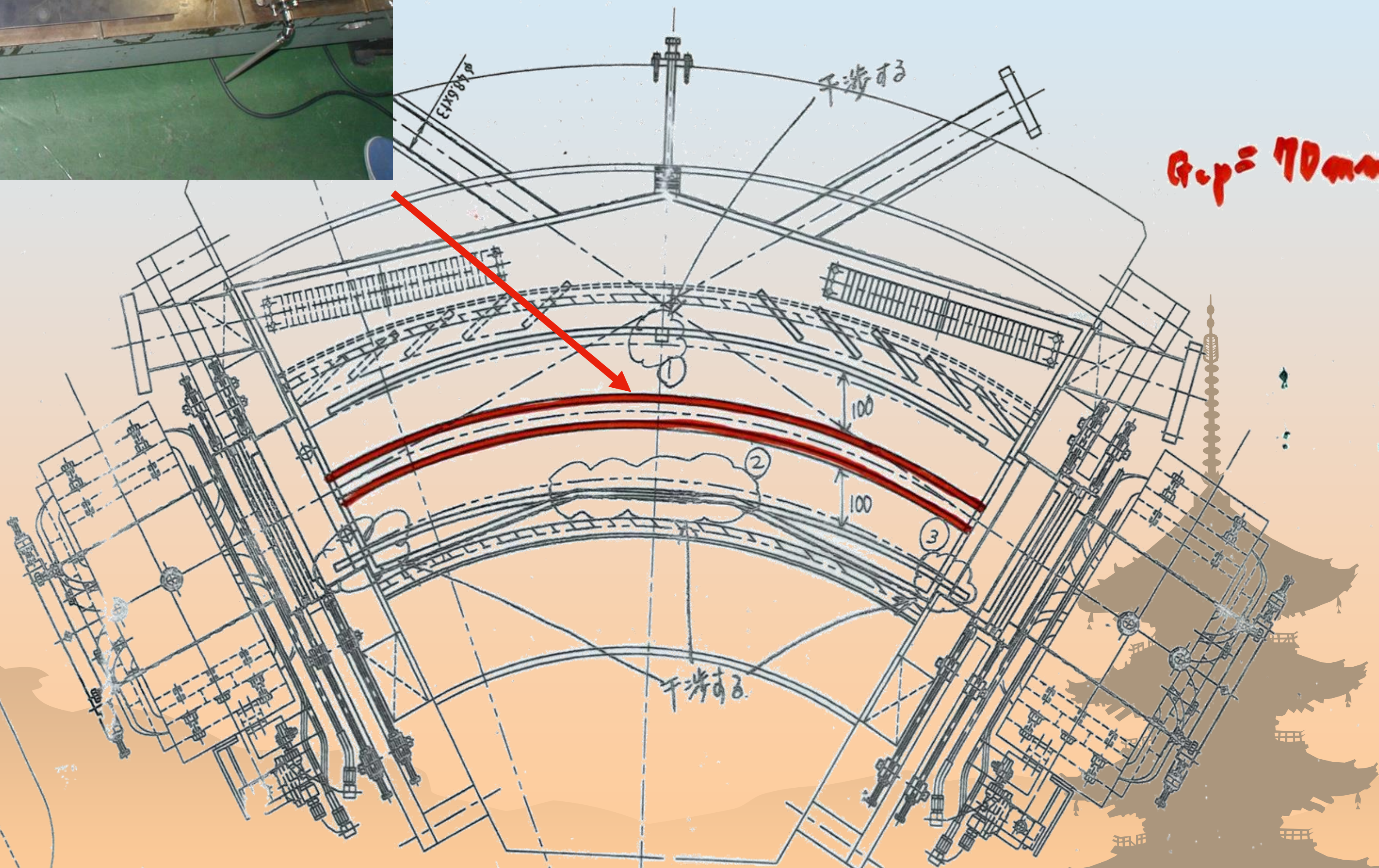

3D Laser Cooling with Dispersion Free Lattice

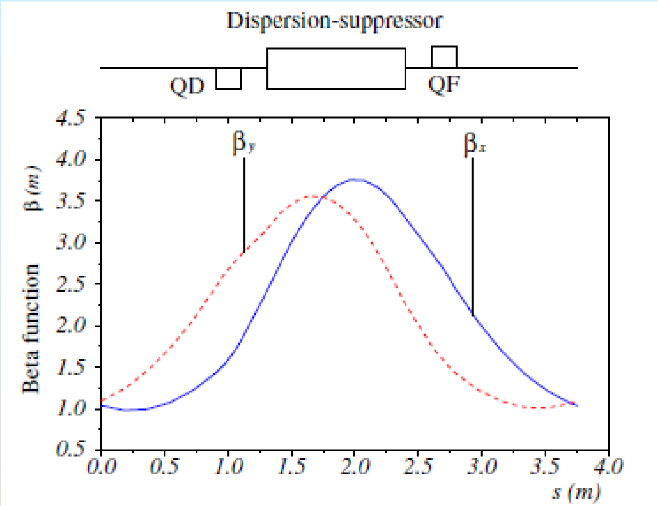

$(\nu_x,\ \nu_y) = (2.07, 2.07)$

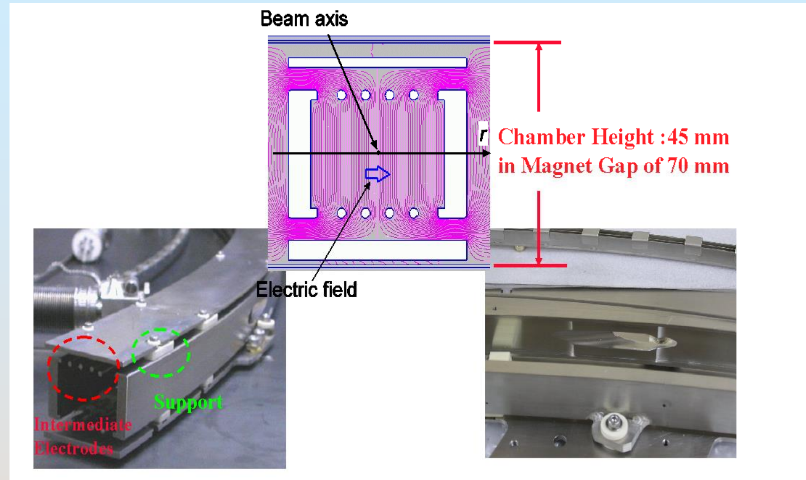

$$2\vec{E} = -(\vec{v} \times \vec{B})$$

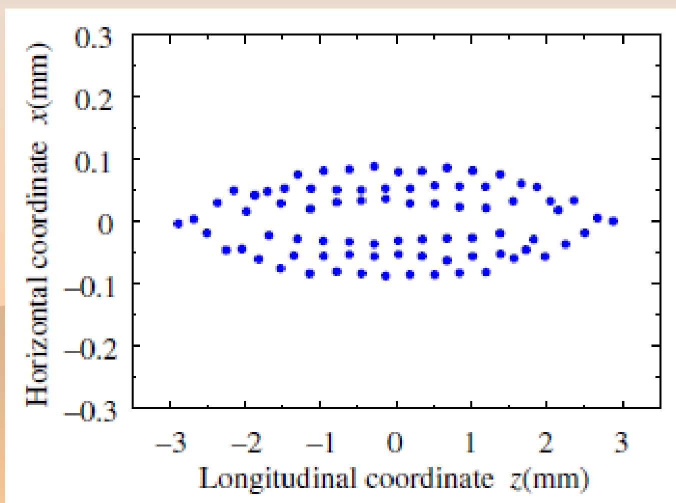

A coupling cavity is needed

To couple the longitudinal and transverse degrees of Freedom.

A few layers 3D crystalline beam is expected.

3 D Laser Cooling + INDAC

Operation Point = (2.068, 1.07)